Journal of Medicinal Chemistry

Article

pubs.acs.org/jmc

Molecular Determinants of Biased Agonism at the Dopamine D_2 Receptor

Dietmar Weichert, Ashutosh Banerjee, Christine Hiller, Ralf C. Kling, Harald Hübner, and Peter Gmeiner*

Department of Chemistry and Pharmacy, Medicinal Chemistry, Emil Fischer Center, Friedrich Alexander University, Schuhstraße 19, 91052 Erlangen, Germany

Supporting Information

ABSTRACT: The development of biased (functionally selective) ligands provides a formidable challenge in medicinal chemistry. In an effort to learn to design functionally selective molecular tools for the highly therapeutically relevant dopamine D_2 receptor, we synthesized a collection of agonists based on structurally distinct head groups derived from canonical or atypical dopaminergic pharmacophores. The test compounds feature a long lipophilic appendage that was shown to mediate biased signaling. By employing functional assays and molecular dynamics simulations, we could show that atypical dopamine surrogates of type **1** and **2** promote biased signaling, while ligands built from classical dopaminergic head groups (type **3** and **4**) typically elicit more balanced signaling profiles. Besides this, we found a strong influence of the stereochemistry of type **4** aminotetraline-derived agonists on functional selectivity at D_2 receptors. Whereas the (*S*)-enantiomer behaved as a full agonist, the biased ligand (*R*)-**4** induced poor G protein coupling but substantial β-arrestin recruitment.

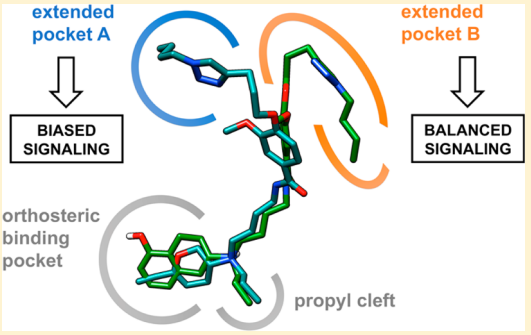

INTRODUCTION

Dopamine D_2 receptors (D_2Rs), which belong to the family A of G protein-coupled receptors (GPCRs), mediate various physiological functions and are involved in a number of neuropsychiatric disorders. Very recent insights from a large genome-wide analysis found an association of psychosis with the D_2 receptor gene DRD2,[1] corroborating the "dopamine hypothesis of schizophrenia".[2] While antagonists or partial agonists are used as antipsychotic drugs, D_2/D_3 receptor agonists are employed to compensate for the lack of cerebral dopamine in case of the Parkinson's disease.[3,4] Two important splice variants of D_2 receptors, namely D_2short (D_{2S}), which is mainly involved in presynaptic dopaminergic transmission, and the postsynaptically localized D_2long (D_{2L}), were identified.[5] Both D_2 isoforms couple promiscuously to $G\alpha_i$ and $G\alpha_o$ subunits of trimeric G proteins and are involved in β-arrestin-mediated internalization and signaling.[3,6] The search for an optimal intrinsic efficacy and ligand selectivity of D_2-addressing drug candidates is further complicated by the growing evidence for a phenomenon referred to as functional selectivity or biased agonism,[7] explaining the capacity of a ligand to preferentially orient the coupling of a GPCR with a subset of signal transducers. Biased signaling may include G protein-mediated effects and G protein-independent responses.[8,9] Very recently, the approved drug aripiprazole and a number of structural modifications were found to serve as biased D_2 receptor ligands.[10−14] The functionally selective test compounds belong to the class of 1,4-disubstituted aromatic piperazines (1,4-DAPs) addressing the orthosteric pocket of the native neurotransmitter dopamine and, additionally, an extended binding area. As a part of our recent effort on the development of novel molecular probes and lead compounds for D_2 and D_3 receptors,[15−19] we reported biased ligands that comprise structurally distinct enyne- and pyrazolo-pyridine-derived head groups and a lipophilic appendage capable to interact with an extended binding site.[15,17] By suggesting that the lipophilic appendages may account for the induction of preferential signaling by addressing particular residues of an extended binding site, we could demonstrate that structurally atypical dopaminergics comprising an enyne moiety and a lipophilic appendage including triazolylalkoxybenzene derivatives are able to discriminate between $G\alpha_{o1}$- and $G\alpha_{i2}$-mediated signaling at D_{2L} and D_{2S} receptors.[16] Interestingly, the crystal structure of the 5-HT_{2B} receptor in complex with the biased agonist ergotamine[20,21] revealed ligand-contacting residues in identical positions, as we suggested by docking studies of D_2 and the functionally selective dopaminergic agent (*S*)-**1** (Figure 1). This finding indicates the potential existence of conserved receptor microdomains that are responsible for ligand bias.

To learn how to rationally design biased GPCR ligands, we planned to hybridize the triazolylalkoxybenzene-derived appendage with both canonical and atypical dopaminergic head groups via an amidobutyl linker and to evaluate such compounds for their binding and functional properties. As a representative dopamine surrogate, we chose a heterocyclic dopamine bioisostere replacing the catechol unit by an 8-hydroxyquinolin-2(1*H*)-one analogue[22] and the 5-hydroxy

Received: December 5, 2014

DOI: 10.1021/jm501889t
J. Med. Chem. XXXX, XXX, XXX−XXX

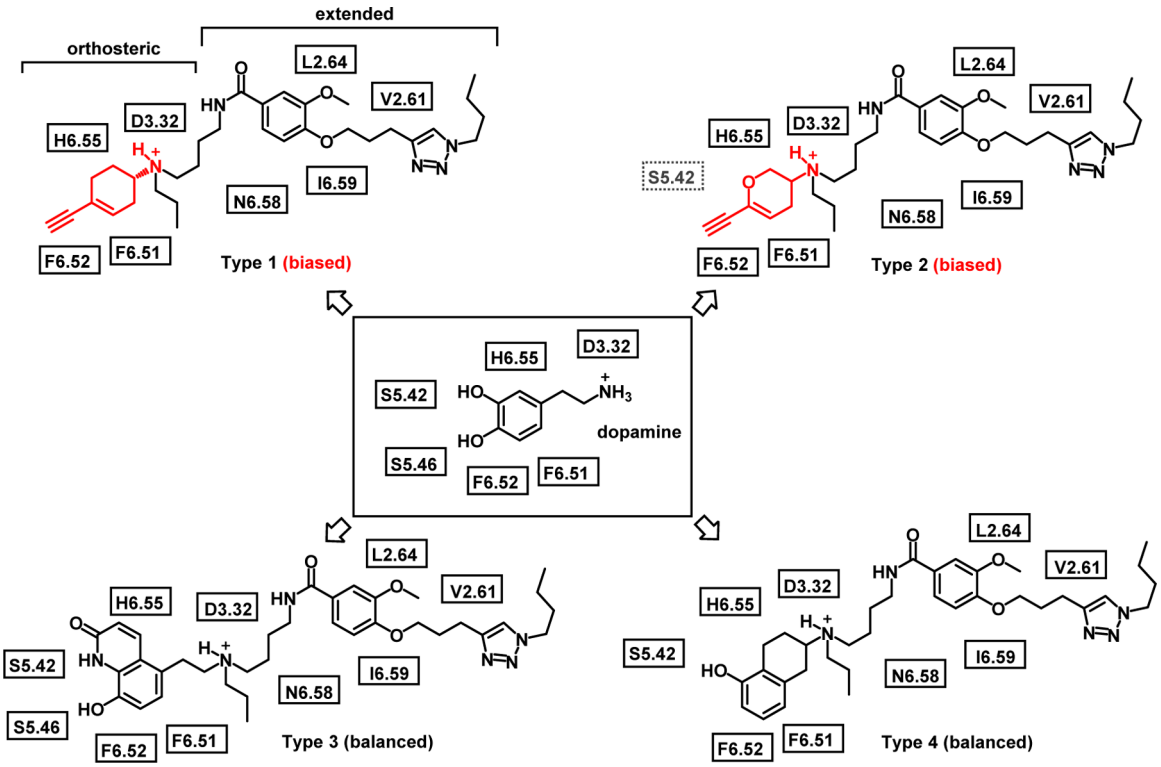

Figure 1. Structures of dopamine as well as the scaffolds of the described ligands of type **1**–**4** are shown and are grouped into potentially biased and more balanced head groups. All compounds occupy the orthosteric binding pocket and form ligand–receptor interactions similar to dopamine. The appendage of the ligands further binds into an extended binding pocket. Representative common interactions are highlighted.

Scheme 1. Synthesis of Type 2 Ligands[a]

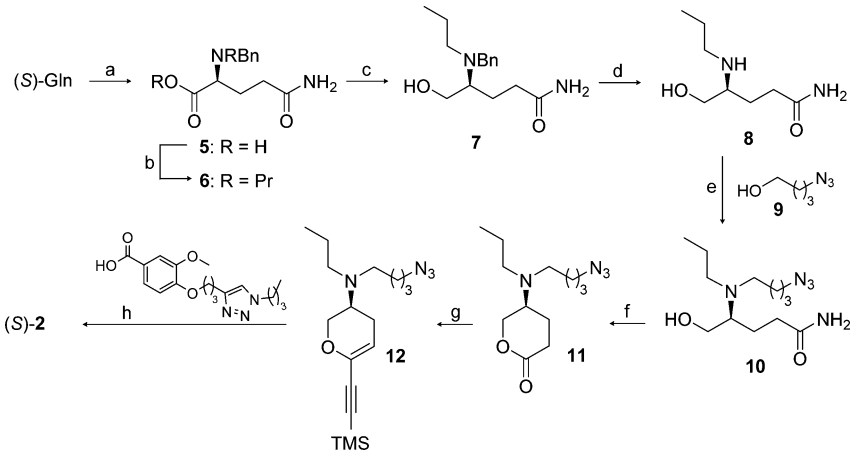

[a]Reagents and conditions: (a) (1) benzaldehyde, NaOH, H_2O/MeOH, rt, 4 h, (2) $NaBH_4$, H_2O/MeOH, 0 °C to rt, 1 h (73%); (b) propyl iodide, DIPEA, DMF/H_2O, 70 °C, 24 h (52%); (c) $LiAlH_4$, THF, −37 °C, 1 h (77%); (d) H_2, Pd/C, MeOH, rt, 5 h (quant); (e) (1) **9**, SO_3·pyridine, Et_3N, CH_2Cl_2/DMSO, 0 °C to rt, 1 h, (2) $NaBH(OAc)_3$, THF, 0 °C to rt, 12 h (88%); (f) toluene, reflux, 3 d (68%); (g) (1) *N*-phenyl-bis(trifluoromethanesulfonimide), KHMDS, THF, −78 °C, 30 min, (2) CuI, $Pd(PPh_3)_2Cl_2$, TMS–acetylene, DMEA, THF, rt, 2 h (64%); (h) (1) PPh_3, THF/H_2O, rt, 24 h, (2) TBTU, DIPEA, CH_2Cl_2, 0 °C to rt, 2 h, (3) TBAF, THF, −25 °C, 30 min (44%); (*R*)-**2** was synthesized from (*R*)-Gln employing identical conditions.

substituted aminotetraline scaffold,[23] leading to the target compounds **3** and (*R*)/(*S*)-**4**, respectively. As an atypical congener, we designed oxa-enynes of type **2**, assuming that the ether oxygen might form a water-mediated H-bond with the side chain of serine 5.42.[24] Such interactions were described to be crucial for receptor activation.[25,26] This work describes the chirospecific synthesis of the dopamine receptor agonists **2**, **3**, and **4** and their investigation for ligand binding, biased signaling, and binding poses in comparison to the functionally selective parent compound (*S*)-**1**.

RESULTS AND DISCUSSION

Synthesis. To enable a comprehensive investigation of their biological activity, both enantiomers of the oxa-enyne test compounds of type **2** were synthesized in pure form, starting from the amino acids (*S*)- and (*R*)-glutamine (Scheme 1). In

DOI: 10.1021/jm501889t
J. Med. Chem. XXXX, XXX, XXX–XXX

detail, (*S*)-glutamine was *N*-monobenzylated by reductive alkylation employing benzaldehyde and sodium borohydride to give the intermediate (*S*)-**5**. The secondary amine and the carboxylic acid function of **5** were alkylated in one step using propyl iodide to afford the carboxylic ester **6**, which was subsequently reduced by $LiAlH_4$ to afford the corresponding alcohol (*S*)-**7**. After hydrogenolysis of the *N*-benzyl protecting group, the aminoalcohol (*S*)-**8** was converted to the tertiary amine (*S*)-**10** by reductive alkylation using freshly prepared 4-azidobutyl aldehyde **9** in the presence of sodium triacetoxyborohydride. Cyclization of (*S*)-**10** gave access to the lactone **11**, which was transformed into the corresponding ketene acetal triflate by α-deprotonation and subsequent reaction with *N*-phenyl-bis(trifluoromethanesulfonimide).[27] Because of the instability of the triflate, the palladium-catalyzed coupling reaction with TMS−acetylene was carried out without further purification resulting in formation of the TMS-protected oxa-enyne (*S*)-**12**. Staudinger reduction of the azide facilitated amide coupling of the primary amine in the presence of TBTU-activated 4-(3-(1-butyl-1*H*-1,2,3-triazol-4-yl)propoxy)-3-methoxybenzoic acid.[16] Upon fluoride-mediated desilylation of the TMS-protecting group, the triazolylalkoxybenzene-substituted oxa-enyne (*S*)-**2** was obtained. The synthesis of the enantiomeric test compound (*R*)-**2** was conducted from (*R*)-glutamine following an identical reaction sequence.

To construct ligands of type **3**, based on a canonical dopamine bioisostere, we started from the commercially available 8-hydroxyquinolin-2(1*H*)-one heterocycle which was *O*-benzyl protected and brominated in position 5 to yield the synthetic intermediate **14** (Scheme 2). The aryl bromide **14**

Scheme 2. Synthesis of Type 3 Ligands[a]

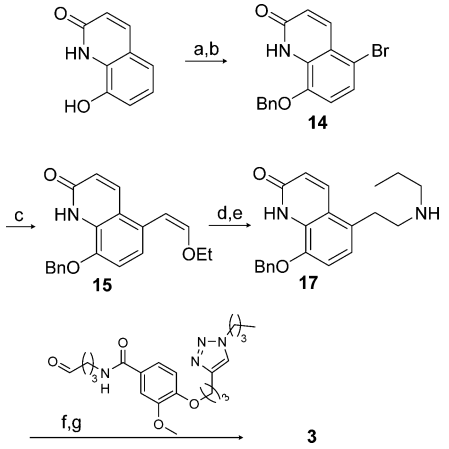

[a]Reagents and conditions: (a) BnBr, K_2CO_3, acetone, reflux, 5 h (88%); (b) Br_2, AcOH, NaOAc, rt, 3 h (73%); (c) Bu_3Sn(*cis*-2-ethoxyethenyl), $Pd(PPh_3)_4$, toluene, 100 °C, 8 h (62%); (d) 2 N HCl/acetone 15:85, reflux, 1 h, crude; (e) *n*-propylamine, $NaBH(OAc)_3$, THF, rt, 16 h (47%); (f) $NaBH(OAc)_3$, THF, rt, 16 h (72%); (g) H_2, 10% Pd/C, MeOH, rt, 20 h (66%).

was subjected to a Stille coupling, leading to the ethoxyethenyl-substituted derivative **15**. The newly introduced functionality served as a masked aldehyde-equivalent, giving access to the corresponding phenylethyl aldehyde upon mild acidic hydrolysis.[28] The aldehyde group was subjected to reductive alkylation using an excess of *n*-propylamine and sodium triacetoxyborohydride to give the secondary amine **17**. Employing a second reductive alkylation reaction, the secondary amine was ligated to the carbaldehyde-substituted lipophilic triazolylalkoxybenzene appendage.[16] Hydrogenolytic cleavage of the benzyl protecting group yielded the target compound **3**.

The synthesis of the aminotetraline derivative of type **4** was performed starting from commercially available (*S*)-5-methoxy-*N*-propyl-2-aminotetraline (Scheme 3). In detail, cleavage of

Scheme 3. Synthesis of Type 4 Ligands[a]

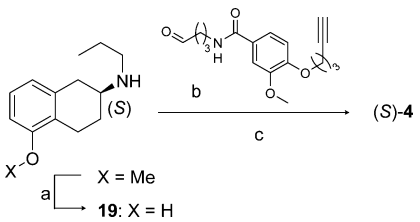

[a]Reagents and conditions: (a) 48% HBr_{aq}, reflux, 16 h, crude; (b) **19**, $NaBH(OAc)_3$, THF, rt, 16 h (80%); (c) *n*-butyl azide, copper(II) sulfate pentahydrate, sodium ascorbate, CH_2Cl_2/MeOH 5:1, rt, 16 h (40%). (*R*)-**4** was synthesized from the enantiomeric building block employing identical conditions.

the methoxy ether using aqueous hydrogen bromide solution afforded the phenol (*S*)-**19**. Subsequent reductive coupling with the lipophilic appendage and reaction with *n*-butyl azide in a copper catalyzed azide−alkyne cycloaddition yielded derivative (*S*)-**4**. The enantiomer (*R*)-**4** was prepared from (*R*)-5-methoxy-*N*-propyl-2-aminotetraline following an identical protocol.

Ligand Binding Experiments. To study the ability of our test compounds featuring structurally distinct head groups to show individual patterns of ligand−receptor interactions, we conducted radioligand displacement assays and compared the results with those obtained for the enyne-derived reference compounds (*R*)- and (*S*)-**1**[16] and the balanced reference agonist quinpirole (Table 1). Binding data were generated by competition binding assays employing [^{3}H]spiperone and cloned human dopamine receptor subtypes D_{2L}, D_{2S}, D_3, and $D_{4.4}$ stably expressed in Chinese hamster ovary (CHO) cells. D_1, D_5 and 5-HT_{2A} receptor affinities were determined using the D_1-selective radioligand [^{3}H]SCH23390 or [^{3}H]ketanserine and cloned human D_1, D_5, and 5-HT_{2A} receptors transiently expressed in HEK 293 cells. For 5-HT_{1A} and α_1 receptor affinities, competition experiments were performed by employing porcine cortical membranes and the selective radioligands [^{3}H]WAY600135 and [^{3}H]prazosin, respectively. Generally, all compounds displayed excellent binding affinity for the isoforms D_{2L} and D_{2S} (K_i values between 0.47 and 53 nM) and for D_3 receptors (K_i values between 0.21 and 2.2 nM) with a preference for the D_3 subtype. The oxa-enynes (*R*)- and (*S*)-**2** showed an approximately 3-fold stereospecific binding at D_{2L}, D_{2S}, and D_3 receptors with a higher affinity for the (*R*)-isomer. These results indicate an analogous binding pose as suggested for the enyne analogues of type **1** when the more potent isomer has to be assigned as (*S*)-**1** due to a reversal of nomenclature exerted by the C,O exchange in the structure.[16] Substantial stereospecific binding was observed for the aminotetralines (*R*)- and (*S*)-**4**. Whereas (*R*)-configuration led to K_i values of 18, 30, and 1.2 nM, (*S*)-**4** exhibited subnanomolar K_i values of 0.47, 0.54, and 0.21 nM for D_{2L}, D_{2S}, and D_3, respectively. The achiral 8-hydroxyquinolin-2(1*H*)-one-derived ligand **3** displayed a significant preference for D_3 over D_{2L} and D_{2S} and,

DOI: 10.1021/jm501889t
J. Med. Chem. XXXX, XXX, XXX−XXX

Table 1. Radioligand Binding Data for the Compounds (*R*)/(*S*)-2, 3, and (*R*)/(*S*)-4 Compared to the Reference Compounds (*R*)/(*S*)-1 and Quinpirole, Employing Human D_1, D_{2L}, D_{2S}, D_3, $D_{4.4}$, D_5 and 5-HT_{2A} Receptors As Well As Porcine 5-HT_{1A} and α_1 Receptors

	K_i ± (SEM) [nM][a]									
	[^{3}H]SCH23390		[^{3}H]spiperone				[^{3}H]WAY100635	[^{3}H]ketanserin	[^{3}H]prazosin	
compd	hD_1	hD_5	hD_{2L}	hD_{2S}	hD_3	$hD_{4.4}$	p5-HT_{1A}	h5-HT_{2A}	$p\alpha_1$	
quinpirole	8700 ± 6000	nd	260 ± 38	70 ± 18	15 ± 3.7	8.5 ± 1.4	6300 ± 1100	25000 ± 920	55000 ± 6200	
(*R*)-**1**	18000 ± 6400[b,c]	nd	14 ± 5.6	8.8 ± 2.2	4.3 ± 1.7	60 ± 18	110 ± 17[b]	28000 ± 13000[b]	1800 ± 350[b]	
(*S*)-**1**	13000 ± 5100[b,c]	nd	9.4 ± 3.5	3.9 ± 1.6	1.0 ± 0.30	30 ± 8.1	160 ± 42[b]	9000 ± 3500[b]	620 ± 160[b]	
(*R*)-**2**	2600 ± 1500[b]	24000 ± 22000[b]	1.6 ± 0.23	2.9 ± 0.78	0.63 ± 0.17	30 ± 4.7	130 ± 59[b]	8000 ± 2300[b]	1000 ± 400[b]	
(*S*)-**2**	3900 ± 0[b]	48000 ± 46000[b]	4.9 ± 1.1	10 ± 0.35	2.2 ± 0.44	180 ± 34	810 ± 78[b]	14000 ± 11000[b]	860 ± 21[b]	
3	4600 ± 600	25000 ± 2900	24 ± 5.0	53 ± 3.2	1.6 ± 0.20	800 ± 170	2800 ± 140[b]	3600 ± 560[b]	2400 ± 160	
(*R*)-**4**	23000 ± 16000[b]	21000 ± 19000[b]	18 ± 3.1	30 ± 5.2	1.2 ± 0.33	290 ± 40	200 ± 7.1[b]	1000 ± 550[b]	480 ± 99[b]	
(*S*)-**4**	2900 ± 1400[b]	700 ± 270[b]	0.47 ± 0.042	0.54 ± 0.063	0.21 ± 0.048	9.4 ± 1.8	22 ± 11[b]	710 ± 130[b]	85 ± 21[b]	

[a] K_i values in nM ± standard error of mean (SEM) derived from 3 to 8 individual experiments each performed in triplicate. nd: not determined. [b] K_i values in nM ± standard deviation (SD) derived from two individual experiments each performed in triplicate. [c] Data obtained using porcine receptors.

in particular, over $D_{4.4}$. Notably, all ligands show moderate or poor affinity at related D_1, as well as the α_1, 5-HT_{1A} and 5-HT_{2A} receptor subtypes.

Functional Experiments. Lefkowitz and co-workers were among the first to describe G protein-independent signaling for the β_2-adrenergic receptor. It was shown that, upon agonist stimulation, β-arrestin can be recruited to the receptor and activate intracellular signaling pathways in a G protein-independent manner.[29] After this phenomenon had been established, biased agonists promoting β-arrestin, but not G protein activation, had been identified for a variety of GPCRs including D_2 receptors.[10,30] However, the molecular basis of functional selectivity still remains elusive.

To facilitate a detailed analysis of the functional properties of the synthesized ligands comprising an atypical oxa-enyne dopamine bioisostere (type **2**) or classical dopaminergic head groups of type **3** and **4**, we performed diagnostic assays. Thus, we investigated the ability of the test compounds to activate pertussis toxin insensitive $G\alpha_i$ or $G\alpha_o$ subunits[31−33] at the D_{2L} and the D_{2S} receptor subtype. Membrane preparations from HEK 293 cells, which were cotransfected with either $G\alpha_{i2}$ or $G\alpha_{o1}$ subunits, were evaluated for ligand-promoted [^{35}S]GTPγS incorporation relative to the nonbiased reference agonist quinpirole.[16,19] Moreover, we employed a β-arrestin recruitment assay using HEK 293 cells transfected with D_{2S}R and β-arrestin-2 that were tagged with complementary fragments of the enzyme β-galactosidase (β-gal). Upon agonist-induced receptor activation, β-arrestin-2 is recruited to the D_{2S} receptor and both fragments of β-gal are combined to restore the activity of the enzyme, which then converts a substrate into a chemiluminescent product, enabling a luminescence-based readout. Quinpirole exhibits virtually identical potencies (EC_{50} values) for coupling to both $G\alpha$ subunits at the long and the short variant of the D_2 receptor (EC_{50} values between 1.6 and 2.8 μM), while the enyne-derived ligand (*S*)-**1** had previously been found to display a preference for $G\alpha_o$ over $G\alpha_i$ activation (Table 2).[16]

To probe the capacity of an oxygen atom bound to an enyne-type scaffold to induce biased signaling, oxa-enyne derivatives of type **2** were evaluated for their activation properties. In fact, the newly developed ligands (*R*)/(*S*)-**2** showed preferential $G\alpha_o$ activation, indicating potency and ligand efficacy similar to the parent compounds (*R*)- and (*S*)-**1**. Interestingly, we observed a distinct activation pattern at D_{2L} receptors for each of the two enantiomers (*R*)-**2** and (*S*)-**2**. The (*R*)-analogue of **2** displayed very similar potencies for $G\alpha_o$ and $G\alpha_i$ coupling but varying E_{max} values of 99% for the $G\alpha_o$-mediated response and only 61% for $G\alpha_i$ activation. Conversely, the preference for $G\alpha_o$ coupling by (*S*)-**2** is characterized by a 21-fold difference in the EC_{50} values of 90 nM for $G\alpha_o$ versus 1900 nM for $G\alpha_i$ activation, with similar maximal effects of 88 and 84%, respectively (Figure 2). Evaluation of β-arrestin recruitment mediated by the oxa-enynes (*R*)- and (*S*)-**2** revealed full activation of this signaling pathway, comparable to their enyne-derived congeners of type **1** (Table 2). Thus, the C,O exchange did not considerably modify the activity profile.

While the above-described biased agonists feature atypical dopaminergic pharmacophores, the ligand based on the classical 8-hydroxyquinolin-2(1*H*)-one catechol surrogate displayed a balanced signaling profile. Test compound **3** showed almost full agonist activity (E_{max} values of 82−87%) and EC_{50} values for G protein activation and β-arrestin recruitment which were similar to the classical reference agent quinpirole (Table

DOI: 10.1021/jm501889t
J. Med. Chem. XXXX, XXX, XXX−XXX

Table 2. Intrinsic Activities and Potencies of Compounds (*R*)/(*S*)-**1**, (*R*)/(*S*)-**2**, **3**, and (*R*)/(*S*)-**4** Determined by [^{35}S]GTPγS Accumulation with Membranes from HEK 293 Cells Transiently Transfected with D_{2S} or D_{2L} and the PTX Resistant $G\alpha_{o1}$ or $G\alpha_{i2}$ G-Protein Subunits and the Recruitment of β-Arrestin-2 after Stimulation of the D_{2S} Receptor

	[^{35}S]GTPγS binding[a]								β-arrestin 2 recruitment[b]	
	D_{2S} $G\alpha_{o1}$		D_{2S} $G\alpha_{i2}$		D_{2L} $G\alpha_{o1}$		D_{2L} $G\alpha_{i2}$		D_{2S}	
compd	EC_{50} [nM]	E_{max} [%][c]	EC_{50} [nM]	E_{max} [%][c]	EC_{50} [nM]	E_{max} [%][c]	EC_{50} [nM]	E_{max} [%][c]	EC_{50} [nM]	E_{max} [%][c]
quinpirole	1600 ± 120	100	2300 ± 470	100	2700 ± 360	100	2800 ± 340	100	83 ± 14	100
(*R*)-**1**	400 ± 100	100 ± 10	2400 ± 1300	76 ± 12	55 ± 14	79 ± 4.4	66 ± 15	73 ± 4.8	140 ± 39	93 ± 2.6
(*S*)-**1**	130 ± 24	104 ± 2.2	1300 ± 690	100 ± 15	92 ± 26	92 ± 2.2	1500 ± 540	76 ± 6.9	16 ± 4.9	93 ± 2.4
(*R*)-**2**	110 ± 37	92 ± 7.3	660 ± 320	94 ± 7.6	52 ± 11	99 ± 11	28 ± 13	61 ± 7.0	380 ± 140	88 ± 7.3
(*S*)-**2**	410 ± 83	108 ± 7.0	2900 ± 720	89 ± 8.8	90 ± 16	88 ± 5.7	1900 ± 540	84 ± 8.7	480 ± 160	101 ± 3.5
3	980 ± 140	87 ± 5.4	1700 ± 960	85 ± 17	3800 ± 1400	82 ± 8.1	7300 ± 3200	84 ± 7.2	140 ± 48	86 ± 7.8
(*R*)-**4**	830 ± 500	27 ± 7.7		<5	530 ± 100	36 ± 6.5		<5	30 ± 16	56 ± 9.7
(*S*)-**4**	2.1 ± 0.17	110 ± 3.5	4.0 ± 1.7	97 ± 2.7	3.1 ± 0.62	90 ± 5.7	2.9 ± 0.50	99 ± 1.8	1.4 ± 0.28	94 ± 3.9

[a]Data represent mean values ± SEM of 3 to 9 individual experiments each performed in triplicate. [b]Data mean values ± SEM of 3 to 18 individual experiments each performed in duplicate. [c]E_{max} displayed as mean values ± SEM are relative (%) to the maximal effect of quinpirole.

2). Accordingly, the aminotetraline headgroup, representing another archetypical dopamine bioisostere, confers (*S*)-**4** full agonist activity (E_{max} values of 90−110%), with excellent potencies in the single-digit nanomolar range in all assays (EC_{50} values of 1.4−4.0 nM).

In stark contrast, investigation of the corresponding (*R*)-enantiomer revealed a remarkably poor G protein coupling. The aminotetraline (*R*)-**4** was not able to activate $G\alpha_i$ protein and induced only marginal $G\alpha_o$ activation to a maximal effect of only 27 and 36% with weak potencies 830 and 530 nM at D_{2S} and D_{2L} receptors, respectively. These results indicate that inversion of the stereochemistry from (*S*) to (*R*) converts compound **4** from being a full agonist for both G protein pathways to an antagonist for $G\alpha_i$ and a low partial agonist for $G\alpha_o$ coupling. Most strikingly, we detected functional selectivity when we investigated (*R*)-**4** for its ability to promote G protein-independent signaling. Although (*R*)-**4** largely prevents G protein coupling, the compound induced substantial β-arrestin recruitment at D_{2S} receptors, revealing 56% ligand efficacy with an EC_{50} value at 30 nM concentration. Consequently, (*R*)-**4** is a remarkably biased agonist toward β-arrestin activation in comparison to $G\alpha_i$ coupling (Figure 2).

Because relative efficacies and potencies are subject to different assay conditions and can be influenced by the respective degree of amplification of the assay systems, we used the operational model of agonism, first derived by Black and Leff,[34] which allows compensation for varying potencies and efficacies of agonists and along pathways. By calculation of a transduction coefficient $\log(\tau/K_A)$ as a measure of the overall agonist efficiency to stimulate particular pathways and normalization of the transduction coefficient to a reference agonist, the resulting $\Delta\log(\tau/K_A)$ values for a given compound can be compared among different pathways to yield the coefficient $\Delta\Delta\log(\tau/K_A)$ as a quantitative measure of ligand bias.[30,35−37] Using quinpirole as a reference agent, the enyne and oxa-enyne derived compounds (*S*)-**1** and (*S*)-**2** indicate substantial bias ($\Delta\Delta\log(\tau/K_A)$ values: 1.37 ± 0.18 and 1.34 ± 0.29), revealing a 23- and 22-fold preference for $G\alpha_o$ over $G\alpha_i$ activation, respectively, at D_{2L} (Supporting Information). Moreover, (*R*)- and (*S*)-**2** display considerable bias toward $G\alpha_o$ coupling over β-arrestin recruitment ($\Delta\Delta\log(\tau/K_A)$ of 1.78 ± 0.22 and 1.41 ± 0.23, respectively). Compound (*R*)-**4** is strongly biased toward β-arrestin- compared to $G\alpha_i$-mediated signaling at the D_{2S} receptor as determined in our activation assays and, thus, bias factors could only be calculated to compare the $G\alpha_o$ and β-arrestin pathway. Despite the notable difference in the maximal effects (56% β-arrestin compared to 27% $G\alpha_o$ activation), application of the operational model indicated a $\Delta\Delta\log(\tau/K_A)$ value of −0.54 ± 0.30.

To verify whether this ligand-specific signaling of compound (*R*)-**4** is partially mediated by the lipophilic triazolylalkoxy-benzene-derived appendage and not solely by the headgroup, we investigated enantiomers of the traditional D_2/D_3 receptor agonist 5-hydroxy-*N*,*N*-dipropyl-2-aminotetraline (5-OH-DPAT).[38] The results showed no preferential activation of either signaling pathways by the propyl-substituted analogues of (*R*)-**4**, indicating that the appendage also is a crucial requirement for biased signaling properties (Supporting Information).

Molecular Dynamics. To discover molecular determinants of biased agonism, binding modes, and ligand−receptor interactions, the dopaminergic test compounds were further investigated. Thus, we used molecular docking to generate initial ligand conformations of the test compounds (*S*)/(*R*)-**2**, **3**, and (*S*)/(*R*)-**4** when bound to our recently developed D_2 receptor model.[16] The conformations were compared to those previously observed for (*S*)-**1** (Supporting Information). Whereas close proximity between the aromatic hydroxyl group of (*S*)-**4** and $Ser^{5.42}$ of the D_2 receptor could be detected, the binding poses of (*S*)/(*R*)-**2** indicated large distance between the oxygen atom of the ligand and $Ser^{5.42}$, explaining that the C,O exchange did not considerably modify the activity profile. These observations were corroborated by mutational studies using $Ser^{5.42}$Ala and $Ser^{5.46}$Ala variants (Supporting Information). Thus, $S^{5.42}$Ala led to significant attenuation of (*S*)-**4** activation but (*S*)-**2** interactions remained unchanged. $Ser^{5.46}$Ala mutation did not negatively affect the potency of the ligands.

Each ligand−receptor complex was submitted to molecular dynamics (MD) simulation runs of 100 ns. RMSD analysis was performed separately for the individual head groups and the appendage moieties of the test compounds, revealing high conformational stability for the head groups throughout the simulation time. In contrast, higher mobility was observed for the appendage units (Supporting Information). Our MD simulations indicate that the lipophilic appendages of the test compounds **3** and (*S*)-**4** undergo conformational changes, thus adopting different conformations compared to those of (*S*)-**1**, (*S*)/(*R*)-**2**, and (*R*)-**4** (Figure 3).

DOI: 10.1021/jm501889t
J. Med. Chem. XXXX, XXX, XXX−XXX

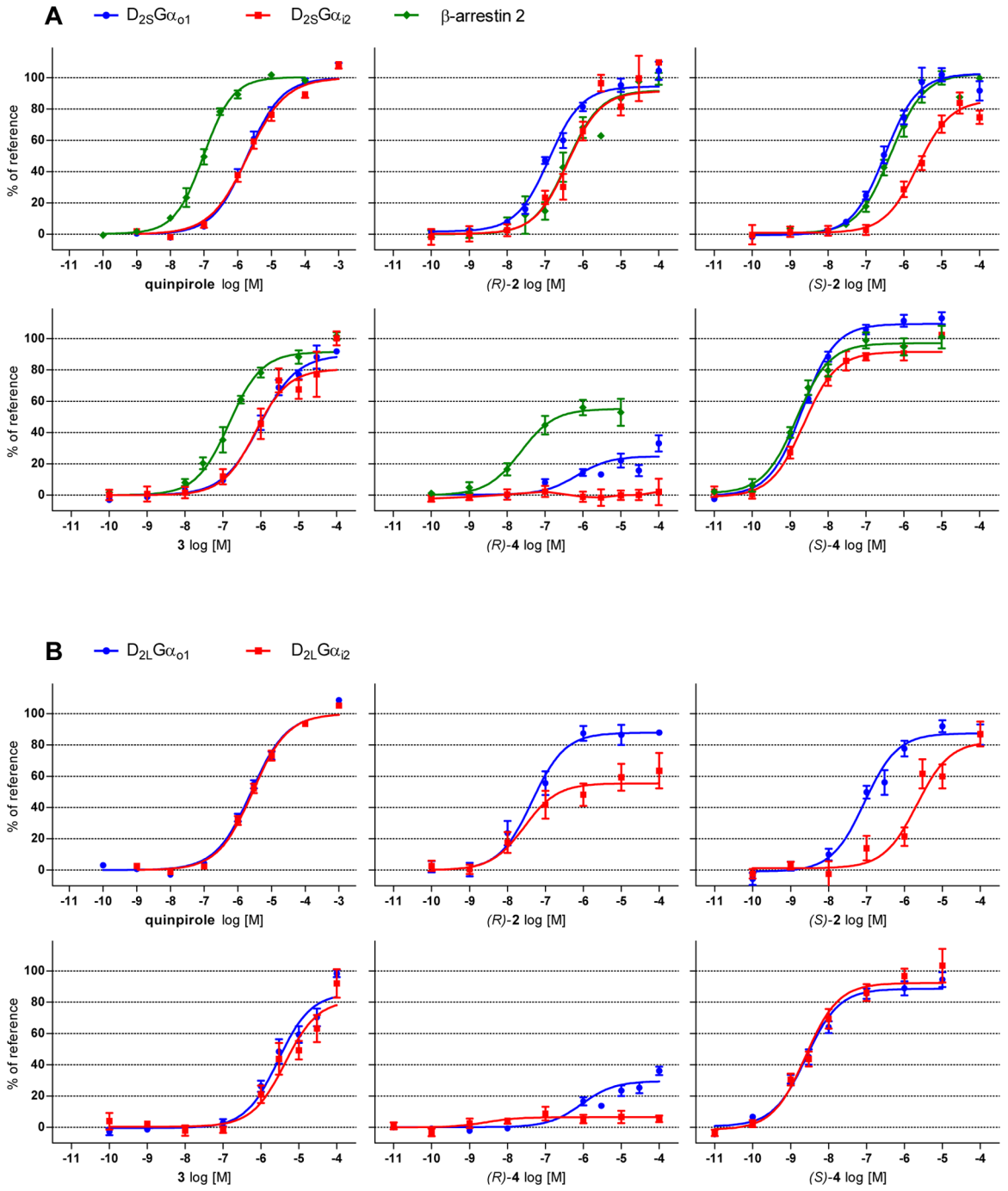

Figure 2. Dose–response curves of the agonist-stimulated [^{35}S]GTPγS binding at D_{2S} and D_{2L} receptors and β-arrestin 2 recruitment at the D_{2S} receptor. (A) D_{2S} receptor activation: membranes from HEK 293 cells transiently transfected with D_{2S} and the PTX insensitive G proteins $G\alpha_{o1}$ or $G\alpha_{i2}$ (D_{2S} + $G\alpha_{o1}$, blue; D_{2S} + $G\alpha_{i2}$, red) or HEK 293-β-arrestin 2 cells transiently transfected with D_{2S}-ARMS2-PK2 (green diamonds) were stimulated with quinpirole, (R)/(S)-**2**, **3**, and (R)/(S)-**4**, respectively. (B) D_{2L} receptor activation: membranes from HEK cells expressing D_{2L} and $G\alpha_{o1}$ or $G\alpha_{i2}$ (D_{2L} + $G\alpha_{o1}$, blue; D_{2L} + $G\alpha_{i2}$, red) were stimulated with quinpirole, (R)/(S)-**2**, **3**, and (R)/(S)-**4**, respectively. All responses were normalized to basal (0%) and the maximum effect of quinpirole (100%).

According to our previous docking investigation on the binding mode of (*S*)-**1** at the D_2 receptor,[16] the appendage of (*S*)-**1** was found to address a region of the extended binding site comparable to that of the biased agonist ergotamine in the crystal structure of the 5-HT_{2B} receptor,[20] in which the appendage units of both (*S*)-**1** at D_2 and ergotamine at 5-HT_{2B} were able to approach homologous residues on top of TM6 including $Asn^{6.58}$ and $Leu^{6.58}$, respectively. We were able to verify the suggested binding mode of (*S*)-**1** by MD simulations (Figure 3). Starting from analogous docking conformations, we observed that (*S*)-**1**, (*S*)/(*R*)-**2**, which differentiate between $G\alpha_o$ and $G\alpha_i$ signaling, and the β-arrestin biased test compound (*R*)-**4**, were able to adopt similar conformations of their appendages after MD refinement, thus maintaining a close proximity to the diagnostic residue $Asn^{6.58}$ above the orthosteric binding pocket of the D_2 receptor. These results support the existence of a conserved receptor microdomain, which can participate in mediating ligand-specific conformations associ-

DOI: 10.1021/jm501889t
J. Med. Chem. XXXX, XXX, XXX−XXX

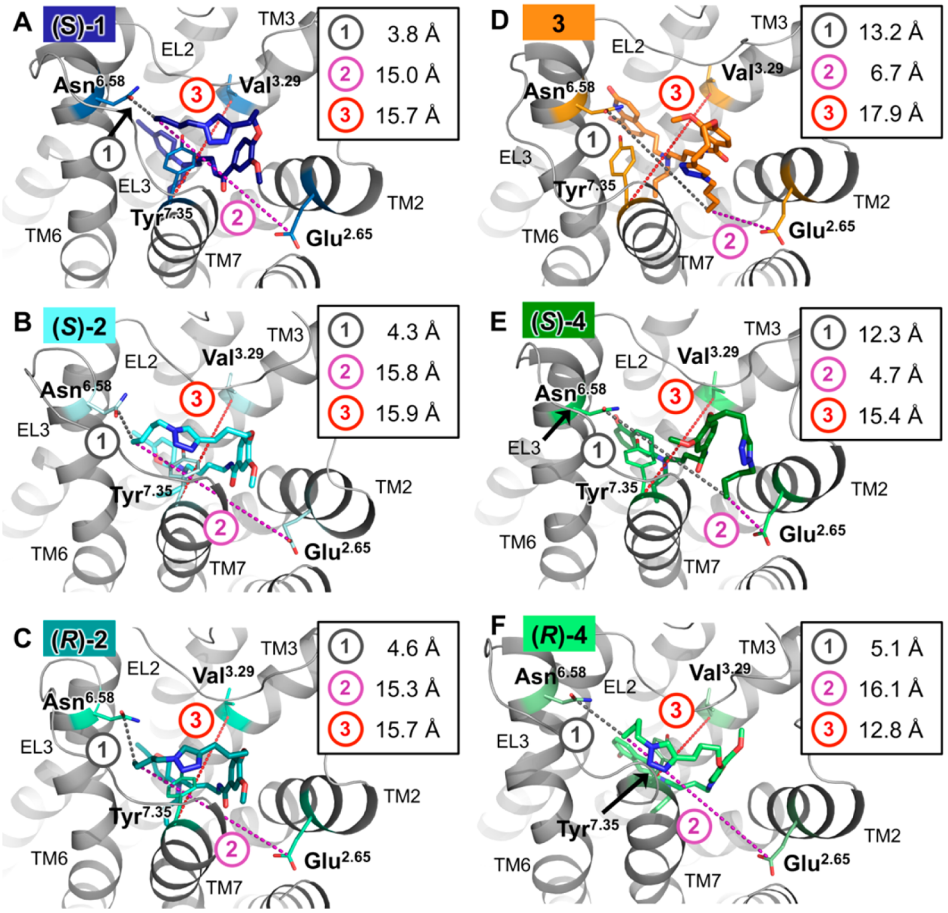

Figure 3. Overview of appendage conformations within the individual MD simulation systems (A–F). Extracellular view on representative snapshots of the test compounds, focusing on the particular conformation of the appendage units of biased and balanced test compounds. The backbone of D_2 is shown as gray ribbons, whereas the diagnostic residues $Glu^{2.65}$, $Val^{3.29}$, $Asn^{6.58}$, and $Tyr^{7.35}$ are represented as sticks. Only the ligands (*S*)-**1** (A, blue), (*S*)-**2** (B, light-cyan), (*R*)-**2** (C, dark-cyan), and (*R*)-**4** (F, light-green) maintained interactions to $Asn^{6.58}$ on top of TM6 (distance 1), whereas the conformation of the appendages of **3** (D) and (*S*)-**4** (E) was found to rearrange toward $Glu^{2.65}$ of TM2 (distance 2). For the (*R*)-**4**-D_2 complex (F), a decrease in the distance between TM3 and TM7 was observed, measured as the Cα–Cα distance between $Val^{3.29}$ and $Tyr^{7.35}$ (distance 3).

ated with biased signaling. Ligands capable of addressing such domains are likely to exhibit a biased signaling profile. In contrast, we detected substantial rearrangements for the appendage units of the test compounds **3** and (*S*)-**4**, both of which activate the investigated pathways with similar potency and efficacy. As a consequence, the appendages of **3** and (*S*)-**4** occupy a topographically distinct binding pocket in the proximity of TM2, which is likely to have, at least in this case, only a minor impact on functionally selective signaling. According to our MD simulations, the β-arrestin-biased aminotetraline (*R*)-**4** showed a particular engagement of the extracellular tip of TM7, leading to a significant inward movement of TM7 displacing residue $Tyr^{7.35}$ closer to TM3. As previous studies suggested TM7 to represent a major structural determinant of β-arrestin-biased signaling,[39−41] it is tempting to assume that the specific rearrangement of TM7 induced by (*R*)-**4** is associated with its preferential β-arrestin activation (Supporting Information).

The general aim of this study was to examine the binding mode of biased D_2 receptor ligands. Our results revealed that the investigated compounds were able to adopt certain binding modes enabling the simultaneous targeting of an orthosteric and an extended binding pocket, which likely interferes with different pathway-specific receptor conformations. This study was not designed to reveal the mechanism, by which a distinct binding mode of biased compounds could be translated into pathway-specific intracellular rearrangements as computational approaches are limited to simulation time restrictions and the availability of full-length crystal structures of GPCR ternary complexes.

CONCLUSION

Functional selectivity constitutes an attractive strategy for the development of drugs associated with reduced side effects.[42−44] Unfortunately, little is known about the molecular determinants accounting for ligand-induced activation of specific signaling pathways at GPCRs and, in particular, the pharmacologically highly relevant D_2 receptor.[30] To learn how to rationally design biased D_2 agonists, we report a series of hybrid compounds comprising atypical or classical dopaminergic head groups and a lipophilic triazolylalkoxybenzene-derived appendage that we identified previously to mediate functional selective signaling of the enyne-derived D_2 agonists (*R*)- and (*S*)-**1**.[16] The target compounds (*R*)/(*S*)-**2**, **3**, and (*R*)/(*S*)-**4** were synthesized in enantiomerically pure form and tested for their functional properties in [^{35}S]GTPγS assays at D_{2S} and D_{2L}Rs and in a β-arrestin recruitment assay at the D_{2S} receptor.

We found that the ligand (*S*)-**2** comprising an atypical oxa-enyne head group served as a biased agonist that displays a

DOI: 10.1021/jm501889t
J. Med. Chem. XXXX, XXX, XXX−XXX

strong preference for $G\alpha_o$ over $G\alpha_i$ activation, which is particularly pronounced at D_{2L} receptors. (*S*)-**2**-type lead compounds might be of interest in drug discovery because activation of $G\alpha_o$ subunits has been suggested to promote synaptic plasticity by stimulating outgrowth of neuronal cells, which is assumed to have an effect on positive symptoms in schizophrenic patients.[45−48] In contrast to atypical dopaminergic head groups, a more balanced signaling profile was observed for classical catechol surrogates of type **3** and for (*S*)-**4**. Most strikingly, we found a remarkable enantiospecific effect on the capacity of compound (*R*)-**4** to differentiate between G protein and β-arrestin signaling. Thus, (*R*)-**4** elicits robust β-arrestin recruitment while being an antagonist for $G\alpha_i$ and a weak partial agonist for $G\alpha_o$ activation. This strong preference for β-arrestin signaling may be of clinical relevance because it was recently shown that β-arrestin biased agonists mediated antipsychotic effects in an animal model for schizophrenia.[12,49]

Our MD simulations indicate that the nature of the head group may allosterically influence the conformation of the appendage moiety, thus affecting the global binding mode of the individual ligand. The binding modes of the biased agonists (*S*)/(*R*)-**2** and (*R*)-**4** corroborate our initial hypothesis on the existence of a conserved receptor microdomain controlling biased agonism. The appendages of the D_2 agonists **3** and (*S*)-**4** were found to occupy a topographically distinct receptor domain, which we suggest to be associated with a more balanced signaling profile.

The newly discovered molecular tools capable of biasing intracellular pathways may be helpful to elucidate the potential of functionally selective D_2 agonists for the treatment of CNS disorders.

EXPERIMENTAL SECTION

Chemistry. Dry solvents and reagents were of commercial quality and were used as purchased. MS were run on a Finnigan MAT TSQ 700 spectrometer by EI (70 eV) with solid inlet or a Bruker Esquire 2000 by APC ionization. HRMS were run on a JEOL JMS-GC Mate II using peak-matching ($M/\Delta M$ > 5000) and on a Bruker Daltonics maXis instrument employing an ESI source. NMR spectra were obtained on a Bruker Avance 360 (^{1}H at 360 MHz, ^{13}C at 90 MHz) or a Bruker Avance 600 (^{1}H at 600 MHz, ^{13}C at 150 MHz) spectrometer in the solvents indicated. Chemical shifts are reported relative to TMS or to the residual solvent peak. Melting points were determined with a MEL-TEMP II melting point apparatus (Laboratory Devices, USA) in open capillaries and are given uncorrected. IR spectra were performed on a Jasco FT/IR 410 spectrometer (film of substance on a NaCl crystal) or on a PerkinElmer Spectrum BX FT-IR (neat). Purification by flash chromatography was performed using Silica Gel 60; TLC analyses were performed using Merck 60 F254 aluminum sheets and the spots were visualized using UV light (254 nm) and reagents such as ninhydrin. Analytical HPLC/MS was performed on Agilent 1100 HPLC systems employing a VWL detector using 254 or 220 nm connected to a Bruker Esquire 2000. The purity of all test compounds and key intermediates was determined by analytical HPLC to be >95% on Agilent 1100 HPLC systems employing a VWL detector using 254 or 220 nm and an Agilent Zorbax SB-C8 (4.6 mm × 150 mm, 5 μm) with a flow rate of 0.5 mL/min (system 1, eluent, methanol/0.1% aq formic acid, 10% methanol for 3 min to 100% methanol in 15 min, 100% for 6 min to 10% in 3 min, 10% for 3 min; system 2, eluent, CH_3CN/0.1% aq formic acid, 5% CH_3CN to 80% in 15 min, to 95% in 1 min, 95% for 3 min, to 5% in 1 min and 5% for 3 min; flow rate, 0.5 mL/min). Preparative HPLC was conducted on an Agilent 1100 Preparative Series, using a Macherey-Nagel Nucleodur C18 HTec (32 mm × 250 mm, 5 μm) column, at a flow of 32 mL/min, with the solvent system indicated.

*(S)-4-(3-(1-Butyl-1H-1,2,3-triazol-4-yl)propoxy)-N-(4-((6-ethynyl-3,4-dihydro-2H-pyran-3-yl)-propylamino)butyl)-3-methoxybenzamide (**2**).* A solution of (*S*)-**12** (18.5 mg, 0.055 mmol) and PPh_3 (115.4 mg, 0.440 mmol) in THF/H_2O (10.0 mL/1.0 mL) was stirred at room temperature for 24 h. After dilution with water, the mixture was frozen and lyophilized. For the acylation reaction, a solution of TBTU (20.5 mg, 0.064 mmol) in dry DMF (0.2 mL) was added dropwise to an ice-cooled solution of 4-(3-(1-butyl-1*H*-1,2,3-triazol-4-yl)propoxy)-3-methoxybenzoic acid[16] (2.0 mg, 0.066 mmol) and DIPEA (23.0 mg, 0.072 mmol) in dry CH_2Cl_2 (2.0 mL). After warming to room temperature, the initially prepared lyophilizate was dissolved in dry CH_2Cl_2 (2.0 mL), was added dropwise to the reaction mixture, and stirred at room temperature for 2 h. The reaction was quenched by adding saturated aqueous $NaHCO_3$, and the product was extracted with CH_2Cl_2. The combined organic layers were dried over $MgSO_4$ and evaporated without heating. The residue was dissolved in THF (5.0 mL) and cooled to −25 °C. A 1 molar solution of TBAF (66 μL, 0.066 mmol) in THF was added slowly and the mixture was stirred for 30 min. After addition of saturated aqueous $NaHCO_3$, the mixture was extracted with CH_2Cl_2, dried ($MgSO_4$), and evaporated without heating. The crude product was purified by HPLC (10−45% acetonitrile/0.1% aq formic acid) to give (*S*)-**2** as white foam (13.4 mg, 44%). IR: 3287, 2937, 2874, 2108, 1684, 1644, 1602, 1581, 1547, 1507, 1464, 1267, 1201, 1177, 1132, 1028, 943, 833 cm^{-1}. ^{1}H NMR (600 MHz, CD_3OD) δ (ppm) 0.94 (t, J = 7.5 Hz, 3 H), 1.01 (t, J = 7.3 Hz, 3 H), 1.27−1.35 (m, 2 H), 1.65−1.90 (m, 8 H), 2.14−2.21 (m, 2 H), 2.50 (ddd, J = 4.5, 4.5,18.9 Hz, 1 H), 2.65 (ddd, J = 5.3, 5.3, 18.9 Hz, 1 H), 2.91 (t, J = 6.7 Hz, 2 H), 3.14−3.26 (m, 2 H), 3.27−3.39 (m, 2 H), 3.45 (t, J = 6.5 Hz, 2 H), 3.52 (s, 1 H), 3.79−3.84 (m, 1 H), 3.89 (s, 3 H), 4.09 (t, J = 6.0 Hz, 2 H), 4.24−4.32 (m, 2 H), 4.36 (t, J = 7.1 Hz, 2 H), 5.37 (t, J = 4.1 Hz, 1 H), 6.99 (d, J = 8.3 Hz, 1 H), 7.44 (dd, J = 2.1, 8.3 Hz, 1 H), 7.46 (d, J = 2.1 Hz, 1 H), 7.83 (s, 1 H). ^{13}C NMR (150 MHz, CD_3OD) δ (ppm) 11.14, 13.74, 19.04, 20.64, 22.75, 22.92, 23.41, 27.89, 29.98, 33.30, 39.59, 51.03, 52.24, 54.01, 56.62, 56.73, 65.14, 69.09, 78.41, 79.13, 107.62, 112.22, 113.42, 121.78, 123.77, 127.87, 138.82, 150.64, 153.01, 169.97. $[\alpha]^{25}_D$ +10.7° (c 0.44, MeOH). HR-EIMS calcd 551.3472; found 551.3472. HPLC: system 1, t_R = 16.0 min, purity 99%; system 2, t_R = 13.5 min, purity 99%. (*R*)-**2** (8.0 mg, 35%, $[\alpha]^{25}_D$ −9.8° (c 0.84, MeOH). HPLC: system 1, t_R = 16.7 min, purity 98%; system 2, t_R = 13.4 min, purity 97%) was prepared from (*R*)-**12** (14.2 mg, 0.042 mmol) as described above for (*S*)-**2**.

*N-(4-((2-(-8-Hydroxy-2-oxo-1,2-dihydroquinolin-5-yl)ethyl)-(propyl)amino)butyl)-4-(3-(1-butyl-1H-1,2,3-triazol-4-yl)propoxy)-3-methoxybenzamide (**3**).* A solution of **18** (22 mg, 0.03 mmol) and 10% Pd/C (3 mg) in anhydrous MeOH (2 mL) was stirred for 20 h under H_2 atmosphere (balloon) at room temperature. The suspension was filtered through Celite, and the filtrate was concentrated in vacuo. The residue was purified by preparative HPLC (6−55% acetonitrile/0.1% aq trifluoroacetic acid) to give **3** as a colorless oil (15 mg, 66% yield). ^{1}H NMR (600 MHz, CD_3OD) δ (ppm) 0.94 (t, J = 7.4 Hz, 3H), 1.04 (t, J = 7.4 Hz, 3H), 1.28−1.34 (m, 2H), 1.72−1.88 (m, 8H), 2.15−2.20 (m, 2H), 2.90−2.93 (m, 2H), 3.19−3.37 (m, 8H), 3.46−3.48 (m, 2H), 4.07−4.09 (m, 2H), 4.36 (t, J = 7.1 Hz, 2H), 6.65 (d, J = 9.7 Hz, 1H), 6.94−6.96 (m, 2H), 7.01−7.02 (m, 1H), 7.39−7.42 (m, 2H), 7.80 (s, 1H), 8.11 (d, J = 9.7 Hz, 1H). ^{13}C NMR (150 MHz, CD_3OD) δ (ppm) 11.15, 13.74, 18.65, 20.64, 21.97, 22.88, 27.01, 27.82, 30.00, 33.32, 39.41, 51.02, 53.85, 54.95, 56.04, 56.57, 69.08, 112.18, 113.37, 115.46, 120.00, 121.75, 122.57, 123.43, 124.91, 125.14, 127.75, 130.00, 138.51, 145.05, 150.61, 153.05, 164.09, 169.96. HR-MS [M$^+$ + 1] calcd 633.3759; found 633.3764. APCI-MS m/z 633.8 [M$^+$ + 1]. HPLC: system 1, t_R = 15.2 min, purity 99.5%; system 2, t_R = 12.0 min, purity 99.5%.

*(S)-4-(3-(1-Butyl-1H-1,2,3-triazol-4-yl)propoxy)-N-(4-((5-hydroxy-1,2,3,4-tetrahydro-naphthalen-2-yl)(propyl)amino)butyl)-3-methoxybenzamide (**4**).* A solution of 3-methoxy-*N*-(4-oxobutyl)-4-(pent-4-yn-1-yloxy)benzamide[50] (63 mg, 0.21 mmol) and **19** (56 mg, 0.27 mmol) in 5 mL of tetrahydrofuran was cooled to 0 °C. Sodium triacetoxyborohydride (89 mg, 0.42 mmol) was added and the reaction warmed to room temperature and stirred for 4 h. The reaction was

DOI: 10.1021/jm501889t
J. Med. Chem. XXXX, XXX, XXX−XXX

quenched with water and extracted with CH_2Cl_2, and the solvent was dried (Na_2SO_4) and evaporated. The crude material was purified by flash chromatography (2−3% MeOH in EtOAc) to afford the (*S*)-isomer of the intermediate alkyne as a yellow oil (79 mg, 80%). ^{1}H NMR (600 MHz, $CDCl_3$): δ (ppm) 0.91 (t, J = 7.3 Hz, 3H), 1.59−1.80 (m, 7H), 1.98 (t, J = 2.7 Hz, 1H), 2.00 (s, 1H), 2.06 (quint, J = 6.7 Hz, 2H), 2.13−2.18 (m, 1H), 2.42 (td, J = 2.6, 6.9 Hz, 2H), 2.44−2.48 (m, 1H), 2.65−2.76 (m, 2H), 2.78−2.95 (m, 5H), 3.20−3.26 (m, 1H), 3.46−3.51 (m, 2H), 3.89 (s, 3H), 4.14 (t, J = 6.3 Hz, 2H), 6.54 (d, J = 8.0 Hz, 1H), 6.67 (d, J = 7.6 Hz, 1H), 6.87 (d, J = 8.2 Hz, 1H), 6.92, (t, J = 7.6 Hz, 1H), 7.09−7.13 (m, 1H), 7.38 (dd, J = 1.9, 8.3 Hz, 1H), 7.48 (d, J = 2.0 Hz, 1H). ^{13}C NMR ($CDCl_3$, 150 MHz): δ (ppm) 11.7, 15.2, 19.9, 23.3, 23.8, 24.0, 24.6, 27.0, 28.0, 30.7, 39.2, 50.0, 52.0, 56.0, 57.7, 67.3, 69.0, 83.3, 111.3, 111.9, 112.4, 119.7, 120.7, 122.7, 126.5, 127.4, 149.3, 151.0, 154.5, 167.4. $[\alpha]^{23}_D$ = −22.0 (*c* 2.20, MeOH). ESI-MS m/z 494.0 [M^+ + 1]. HPLC: t_R = 16.0 min, purity 99%. The (*R*)-isomer of the intermediate alkyne (147.5 mg, 92%, $[\alpha]^{26}_D$ = +25.8 °C (*c* 1.13, MeOH)) was prepared from (*R*)-**19** (73.7 mg, 0.36 mmol) as described above. A solution of the alkyne (38 mg, 0.08 mmol), 1-azidobutane (6 mg, 0.06 mmol), copper(II) sulfate pentahydrate (15 mg, 0.06 mmol), and sodium ascorbate (35 mg, 0.18 mmol) in 5 mL of CH_2Cl_2 and 1 mL of methanol was stirred overnight at room temperature. The reaction was quenched with water and extracted with CH_2Cl_2. The solvent was dried using sodium sulfate and evaporated in vacuo. The crude material was purified by HPLC (40−80% methanol/0.1% aq formic acid) to afford (*S*)-**4** a white solid (16 mg, 46%). ^{1}H NMR (600 MHz, $(CD_3)_2SO$) δ (ppm) 0.81−0.91 (m, 6H), 1.22 (sextet, J = 7.6 Hz, 2H), 1.38−1.59 (m, 7H), 1.76 (quint, J = 7.3 Hz, 2H), 1.94−2.00 (m, 1H), 2.05 (quint, J = 7.2 Hz, 2H), 2.36−2.45 (m, 1H), 2.48−2.54 (3H, overlaid by DMSO signal), 2.59 (t, J = 6.8 Hz, 2H), 2.64−2.86 (m, 5H), 2.88−2.95 (m, 1H), 3.25 (q, J = 6.0 Hz, 2H), 3.80 (s, 3H), 4.04 (t, J = 6.2 Hz, 2H), 4.28 (t, J = 7.1 Hz, 2H), 6.50 (d, J = 7.6 Hz, 1H), 6.57 (d, J = 7.8 Hz, 1H), 6.86 (t, J = 7.7 Hz, 1H), 6.96 (d, J = 8.7 Hz, 1H), 7.41−7.45 (m, 2H), 7.89 (s, 1H), 8.32 (t, J = 5.5 Hz, 1H). ^{13}C NMR (150 MHz, $(CD_3)_2SO$) δ (ppm) 11.65, 13.26, 19.06, 21.11, 21.58, 23.41, 24.79, 25.36, 27.03, 28.45, 31.42, 31.68, 48.84, 49.56, 51.67, 55.58, 56.25, 67.44, 110.86, 111.52, 111.88, 119.72, 120.25, 121.81, 122.76, 125.89, 127.04, 137.20, 146.02, 148.34, 150.35, 154.75, 165.55 (one carbon peak overlaid by DMSO signal). $[\alpha]^{23}_D$ = −21.6 (*c* 0.91, MeOH). HR-EIMS calcd 591.3785; found 591.3785. ESI-MS m/z 593.0 [M^+ + 1]. HPLC: system 1, t_R = 16.2 min, purity 100%; system 2 t_R = 12.4 min, purity 97%. (*R*)-**4** (9 mg, 40%, $[\alpha]^{25}_D$ = −21.6 (*c* 0.91, MeOH). HPLC: system 1, t_R = 16.0 min, purity 98%; system 2, t_R = 12.3 min, purity 98%) was prepared from the (*R*)-isomer of the intermediate alkyne (18 mg, 0.04 mml) and 1-azidobutane (5 mg, 0.05 mmol) as described for (*S*)-**4**.

*(S)-N-Benzylglutamine (**5**).* Benzaldehyde (8.2 mL, 80.8 mmol) was added dropwise to a solution of (*S*)-glutamine (5.90 g, 40.4 mmol) and NaOH (1.62 g, 40.4 mmol) in a 7:3 mixture of H_2O and MeOH (100.0 mL), and the reaction was stirred at room temperature for 4 h.[51] After cooling the reaction mixture to 0 °C and addition of $NaBH_4$ (1.83 g, 48.5 mmol), the reaction was stirred at room temperature for 1 h. Then the solution was acidified by adding glacial acid until the product precipitated. The product was filtered off, washed, and dried ($MgSO_4$) to give (*S*)-**5** as a white solid (6.97 g, 73%); mp 200 °C. ^{1}H NMR (600 MHz, pyridin-d_5/D_2O) δ (ppm) 1.72−1.85 (m, 2 H), 2.05−2.14 (m, 2 H), 3.29 (dd, J = 5.8, 6.7 Hz, 1 H), 3.66 (d, J = 12.8 Hz, 1 H), 3.76 (d, J = 12.8 Hz, 1 H), 6.72−6.76 (m, 1 H), 6.79−6.83 (m, 2 H), 6.97−6.02 (m, 2 H). ^{13}C NMR (150 MHz, pyridin-d_5/D_2O) δ (ppm) 27.73, 33.18, 52.17, 63.51, 125.09, 130.81, 130.88, 131.62, 133.58, 138.18, 174.94, 179.07. APCI-MS m/z 237.0 [M^+ + 1]. (*R*)-**5** (6.41 g, 79%) was prepared from (*R*)-glutamine (5.04 g, 34.5 mmol) as described above for (*S*)-**5**.

*(S)-Propyl 5-Amino-2-(N-benzyl-N-propylamino)-5-oxopenanoate (**6**).* To a solution of (*S*)-**5** (2.33 g, 9.84 mmol) in DMF/H_2O (70.0 mL/25.0 mL), DIPEA (16.7 mL, 98.40 mmol) and propyl iodide (14.3 mL, 147.60 mmol) were added successively. The reaction mixture was stirred at 70 °C for 24 h. After addition of saturated aqueous $NaHCO_3$ and basification with 6 N NaOH, the aqueous layer was extracted with diethyl ether. The combined organic layers were dried ($MgSO_4$), and the solvent was evaporated. The crude product was purified by column chromatography (hexane/EtOAc 1:1) to afford (*S*)-**6** as a yellowish oil (1.64 g, 52%). IR: 3445, 3349, 3193, 3086, 3064, 3030, 2964, 2875, 1726, 1668, 1621, 1493, 1455, 1403, 1310, 1239, 1205, 1165, 1136, 1101, 1060, 1028, 967, 906 cm^{-1}. ^{1}H NMR (600 MHz, $CDCl_3$) δ (ppm) 0.87 (t, J = 7.4 Hz, 3 H), 0.99 (t, J = 7.5 Hz, 3 H), 1.41−1.59 (m, 2 H), 1.68−1.74 (m, 2 H), 1.91−1.97 (m, 1 H), 2.00−2.05 (m, 1 H), 2.17 (ddd, J = 7.6, 7.6, 15.0 Hz, 1 H), 2.29 (ddd, J = 6.3, 8.0, 14.9 Hz, 1 H), 2.49 (ddd, J = 4.5, 8.5, 13.0 Hz, 1 H), 2.59 (ddd, J = 8.0, 8.0, 12.9 Hz, 1 H), 3.32 (dd, J = 5.5, 9.6 Hz, 1 H), 3.60 (d, J = 13.9 Hz, 1 H), 3.90 (d, J = 13.9 Hz, 1 H), 4.08 (dt, J = 6.7, 10.7 Hz, 1 H), 4.12 (dt, J = 6.7, 10.7 Hz, 1H), 7.20−7.36 (m, 5 H). ^{13}C NMR (90 MHz, $CDCl_3$) δ (ppm) 10.63, 11.70, 21.71, 22.17, 25.24, 32.22, 52.52, 55.27, 61.16, 65.90, 126.96, 128.27, 128.97, 140.11, 172.74, 174.75. APCI-MS m/z 321.2 [M^+ + 1]. $[\alpha]^{29}_D$ −104.7° (*c* 1.16, $CHCl_3$). (*R*)-**6** (1.73 g, 55%, $[\alpha]^{21}_D$ +106.3° (*c* 1.66, $CHCl_3$)) was prepared from (*R*)-**5** (2.33 g, 9.84 mmol) as described above for (*S*)-**6**.

*(S)-4-(Benzylpropylamino)-5-hydroxypentanamide (**7**).* A solution of (*S*)-**6** (1.01 g, 3.15 mmol) in THF (30.00 mL) was cooled to −37 °C, and a 2.4 M solution of $LiAlH_4$ in THF (1.97 mL, 4.74 mmol) was added slowly. After stirring at −37 °C for 1 h, the reaction was quenched by careful addition of aqueous $NaHCO_3$. The resulting suspension was filtered through a pad of Celite, the filtrate was concentrated, and the residue was purified by flash chromatography (CH_2Cl_2/MeOH saturated with NH_3 40:1) to isolate (*S*)-**7** as yellowish oil (639.5 mg, 77%). IR: 3350, 3196, 3086, 3062, 3027, 2958, 2871, 2823, 1666, 1617, 1493, 1455, 1408, 1322, 1259, 1134, 1028 cm^{-1}. ^{1}H NMR (600 MHz, $CDCl_3$) δ (ppm) 0.84 (t, J = 7.4 Hz, 3 H), 1.43 (dddd, J = 6.9, 8.3, 13.3, 14.9 Hz, 1 H), 1.47−1.56 (m, 2 H), 2.04 (dddd, J = 4.3, 6.7, 9.4, 13.7 Hz, 1 H), 2.15 (ddd, J = 6.7, 8.7, 15.3 Hz, 1 H), 2.21 (ddd, J = 6.2, 9.2, 15.3 Hz, 1 H), 2.43−2.52 (m, 2 H), 2.76 (dddd, J = 4.4, 5.1, 9.5, 9.5 Hz, 1 H), 3.24 (s, 1 H), 3.40 (dd, J = 10.2, 10.2 Hz, 1 H), 3.48 (d, J = 13.6 Hz, 1 H), 3.49 (dd, J = 5.2, 10.4 Hz, 1 H), 3.80 (d, J = 13.6 Hz, 1 H), 5.45 (s, 2 H), 7.23−7.33 (m, 5 H). ^{13}C NMR (90 MHz, $CDCl_3$) δ (ppm) 11.67, 21.22, 21.83, 32.91, 51.04, 54.04, 59.95, 60.80, 127.08, 128.40, 128.90, 139.73, 174.47. APCI-MS m/z 265.1 [M^+ + 1]. $[\alpha]^{30}_D$ +75.9° (*c* 1.19, $CHCl_3$). (*R*)-**7** (1.00 g, 71%, $[\alpha]^{25}_D$ −74.3° (*c* 0.96, $CHCl_3$)) was prepared from (*R*)-**6** (1.71 g, 5.34 mmol) as described above for (*S*)-**7**.

*(S)-5-Hydroxy-4-(propylamino)pentanamide (**8**).* A mixture of (*S*)-**7** (1.0 g, 3.79 mmol) and 10% Pd/C in MeOH (40 mL) was stirred at room temperature under H_2 atmosphere (balloon) for 5 h. Then, the catalyst was removed by filtration through a pad of Celite, and the solvent was evaporated to afford (*S*)-**8** as a white solid (665.1 mg, quant); mp 99 °C. IR: 3305, 3186, 2958, 2930, 2870, 1668, 1537, 1456, 1410, 1358, 1291, 1123, 1043, 991 cm^{-1}. ^{1}H NMR (600 MHz, CD_3OD) δ (ppm) 0.95 (t, J = 7.4 Hz, 3 H), 1.48−1.57 (m, 2 H), 1.68 (dddd, J = 6.8, 7.0, 8.7, 14.0 Hz, 1 H), 1.79 (dddd, J = 5.2, 7.0, 8.8, 14.0 Hz, 1 H), 2.25 (ddd, J = 7.0, 8.6, 14.7 Hz, 1 H), 2.28 (ddd, J = 6.6, 8.7, 14.8 Hz, 1 H), 2.53−2.64 (m, 3 H), 3.43 (dd, J = 6.4, 11.1 Hz, 1 H), 3.60 (dd, J = 4.7, 11.1 Hz, 1 H). ^{13}C NMR (90 MHz, CD_3OD) δ (ppm) 12.00, 23.83, 27.77, 32.98, 49.88, 60.07, 63.82, 178.75. APCI-MS m/z 175.0 [M^+ + 1]. $[\alpha]^{30}_D$ +18.8° (*c* 0.76, MeOH). (*R*)-**8** (586.1 mg, 90%, $[\alpha]^{25}_D$ −19.4° (*c* 1.03, MeOH)) was prepared from (*R*)-**7** (990.3 mg, 3.75 mmol) as described above for (*S*)-**8**.

*4-Azidobutanol (**9**).* To an ice-cold suspension of $NaBH_4$ (839.8 mg, 22.2 mmol) in dry THF (60 mL) a solution of I_2 (9.39 g, 97.0 mmol) in THF (24 mL) was added slowly under N_2 atmosphere. After stirring at room temperature for 3 h, a solution of NaN_3 (9.62 g, 148.0 mmol) in H_2O (20 mL) was added dropwise and the reaction mixture was stirred for 24 h. Then the mixture was diluted with H_2O (50 mL) and extracted with diethyl ether. The combined organic layers were washed successively with aqueous $Na_2S_2O_3$, H_2O, and brine and subsequently dried using $MgSO_4$. The solvents were evaporated at 32 °C to furnish **9** as yellowish oil (4.03 g, 95%). Analytical data as described in literature.[52]

*(S)-4-((4-Azidobutyl)propylamino)-5-hydroxypentanamide (**10**).* To an ice-cold solution of **9** (959.3 mg, 8.33 mmol) in CH_2Cl_2/DMSO (8.0 mL/4.0 mL), Et_3N (4.6 mL, 33.30 mmol), and SO_3·

DOI: 10.1021/jm501889t
J. Med. Chem. XXXX, XXX, XXX−XXX

pyridine (7.64 g, 25.00 mmol) were added. After being stirred at room temperature for 1 h, the mixture was diluted with H_2O and extracted with CH_2Cl_2. The combined organic layers were washed with 2 N HCl_{aq}, H_2O, and brine, dried ($MgSO_4$), and concentrated.

The residue was diluted with THF (20.0 mL) and added dropwise to an ice-cold solution of (*S*)-**8** (353.3 mg, 2.03 mmol) in THF (50.0 mL). Then $NaBH(OAc)_3$ (2.15 g, 10.20 mmol) was added in one portion at 0 °C. The suspension was allowed to warm to room temperature and was stirred for 12 h. The reaction was terminated by addition of saturated aqueous $NaHCO_3$, and the aqueous layer was extracted with CH_2Cl_2. The combined organic layers were dried ($MgSO_4$), and the solvent was removed in vacuo. The resulting residue was purified using column chromatography (CH_2Cl_2 + 5% MeOH saturated with NH_3) to give (*S*)-**10** as yellow oil (486 mg, 88%). IR: 3344, 3199, 2956, 2870, 2097, 1667, 1618, 1460, 1408, 1348, 1257, 1166, 1142, 1035, 890 cm^{-1}. ^1H NMR (600 MHz, $CDCl_3$) δ (ppm) 0.89 (t, J = 7.4 Hz, 3 H), 1.37−1.67 (m, 7 H), 1.94 (dddd, J = 4.4, 6.8, 9.3, 14.0 Hz, 1 H), 2.18 (ddd, J = 6.8, 8.6, 15.3 Hz, 1 H), 2.23 (ddd, J = 6.1, 9.2, 15.3 Hz, 1 H), 2.39 (ddd, J = 4.6, 8.5, 13.1 Hz, 1 H), 2.43−2.49 (m, 2 H), 2.54 (ddd, J = 7.1, 8.4, 13.0 Hz, 1 H), 2.76 (dddd, J = 4.8, 4.8, 9.6, 9.6 Hz, 1 H), 3.29 (t, J = 6.4 Hz, 1 H), 3.30 (dd, J = 10.1, 10.5 Hz, 1 H), 3.50 (dd, J = 5.2, 10.5 Hz, 1 H), 5.47 (s, 2 H). ^{13}C NMR (150 MHz, $CDCl_3$) δ (ppm) 11.73, 21.29, 22.24, 26.35, 26.69, 32.85, 49.34, 51.34, 51.55, 60.68, 60.99, 174.39. APCI-MS m/z 272.1 [M^+ + 1]. $[\alpha]^{29}_D$ +34.5° (c 1.35, $CHCl_3$). (*R*)-**10** (656.5 mg, 72%, $[\alpha]^{21}_D$ −38.2° (c 0.90, $CHCl_3$)) was prepared from (*R*)-**8** (586.1 mg, 3.36 mmol) as described above for (*S*)-**10**.

*(S)-5-((4-Azidobutyl)propylamino)tetrahydro-2H-pyran-2-one (**11**).* A solution of (*S*)-**10** (526.9 mg, 1.94 mmol) in toluene (40 mL) was refluxed for 3 d. The solvent was removed under reduced pressure, and the resulting residue was purified by flash chromatography (hexane/EtOAc 2:1) to afford (*S*)-**11** as yellow oil (335.5 mg, 68%). IR: 2957, 2871, 2814, 2095, 1744, 1458, 1378, 1253, 1177, 1054, 912 cm^{-1}. ^1H NMR (600 MHz, $CDCl_3$) δ (ppm) 0.88 (t, J = 7.3 Hz, 3 H), 1.38−1.65 (m, 6 H), 1.86 (dddd, J = 6.8, 8.9, 8.9, 13.6 Hz, 1 H), 1.98−2.04 (m, 1 H), 2.40−2.55 (m, 5 H), 2.66 (ddd, J = 5.9, 6.7, 17.1 Hz, 1 H), 3.13 (dddd, J = 5.0, 6.1, 7.7, 8.8 Hz, 1 H), 3.29 (t, J = 6.8, 2 H), 4.19 (dd, J = 7.7, 11.5 Hz, 1 H), 4.28 (ddd, J = 1.2, 5.0, 11.5 Hz, 1 H). ^{13}C NMR (150 MHz, $CDCl_3$) δ (ppm) 11.65, 21.28, 21.44, 25.57, 26.60, 28.71, 50.06, 51.39, 52.45, 53.43, 69.59, 171.68. APCI-MS m/z 255.1 [M^+ + 1]. $[\alpha]^{29}_D$ +11.6° (c 2.39, $CHCl_3$). (*R*)-**11** (357.0 mg, 58%, $[\alpha]^{21}_D$ −10.3° (c 1.26, $CHCl_3$)) was prepared from (*R*)-**10** (652.7 mg, 2.41 mmol) as described above for (*S*)-**11**.

*(S)-N-(4-Azidobutyl)-N-propyl-(6-(trimethylsilyl)ethynyl-3,4-dihydro-2H-pyran-3-yl)amine (**12**).* A solution of (*S*)-**11** (84.1 mg, 0.33 mmol) and *N*-phenyl-bis(trifluoromethanesulfonimide) (590.6 mg, 1.65 mmol) in dry THF (20.00 mL) was cooled to −78 °C, and a 0.7 M solution of KHMDS in toluene (2.36 mL, 1.65 mmol) was added dropwise. After being stirred for 30 min, the reaction was quenched by addition of DMEA (0.72 mL, 6.62 mmol). The solution was allowed to warm to room temperature and concentrated under reduced pressure without heating. Then the residue was dissolved in THF (10.00 mL), and CuI (12.6 mg, 0.066 mmol) and $Pd(PPh_3)_2Cl_2$ (11.6 mg, 0.016 mmol) were added. After subsequent addition of TMS−acetylene (0.14 mL, 0.99 mmol) and DMEA (0.36 mL, 3.31 mmol), the reaction mixture was stirred at room temperature for 2 h. The reaction was quenched by the addition of saturated aqueous $NaHCO_3$, and the aqueous layer was extracted with CH_2Cl_2. The combined organic layers were dried ($MgSO_4$) and evaporated without heating. Purification of the resulting residue by HPLC (acetonitrile/H_2O + 0.1% HCOOH) yielded (*S*)-**12** as yellowish oil (70.3 mg, 64%). IR: 2958, 2872, 2814, 2158, 2095, 1635, 1462, 1375, 1336, 1282, 1249, 1189, 1044, 995, 860, 843 cm^{-1}. ^1H NMR (360 MHz, $CDCl_3$) δ (ppm) 0.19 (s, 9 H), 0.86 (t, J = 7.4 Hz, 3 H), 1.36−1.64 (m, 6 H), 2.12−2.16 (m, 2 H), 2.39−2.51 (m, 4 H), 2.95−3.04 (m, 1 H), 3.27 (t, J = 6.8 Hz, 2 H), 3.64 (t, J = 10.2 Hz), 4.11−4.15 (m, 1 H), 5.26−5.28 (m, 1 H). ^{13}C NMR (90 MHz, $CDCl_3$) δ (ppm) 0.29, 11.66, 21.92, 24.33, 25.95, 26.60, 50.11, 51.45, 52.55, 52.70, 67.97, 93.09, 99.39, 108.59, 136.85. APCI-MS m/z 335.2 [M^+ + 1]. $[\alpha]^{17}_D$ +32.6° (c 0.91, $CHCl_3$). (*R*)-**12** (41.5 mg, 57%, $[\alpha]^{17}_D$ −30.3° (c 0.94, $CHCl_3$)) was prepared from (*R*)-**11** (55.7 mg, 0.22 mmol) as described above for (*S*)-**12**.

*8-(Benzyloxy)quinolin-2(1H)-one (**13**).* Benzyl bromide (810 μL, 6.8 mmol) was added to a suspension of 8-hydroxyquinolin-2(1*H*)-one (1.0 g, 6.2 mmol) and K_2CO_3 (1.2 g, 8.7 mmol) in acetone (30 mL). After being stirred at reflux for 5 h, the mixture was allowed to cool to room temperature and the solvent was evaporated. The residue was suspended in H_2O and extracted with CH_2Cl_2. The combined organic layers were dried (Na_2SO_4), filtered, and evaporated. The crude material was purified by flash chromatography (hexane/EtOAc 1:1) to give **13** as a white solid (1.4 g, 88% yield). Analytical data as described in literature.[53]

*8-(Benzyloxy)-5-bromoquinolin-2(1H)-one (**14**).* A solution of bromine (280 μL, 5.44 mmol) in glacial acetic acid (6 mL) was added dropwise to a solution of **13** (1.37 g, 5.44 mmol) and sodium acetate (1.48 g, 18.00 mmol) in glacial acetic acid (25 mL) at room temperature. The reaction mixture was stirred at room temperature for 3 h. Then the solvent was evaporated and the residue was purified by flash chromatography (cyclohexane/EtOAc 7:3) to give **14** as white solid (1.31 g, 73% yield). Analytical data as described in literature.[53]

*(Z)-8-(Benzyloxy)-5-(2-ethoxyvinyl)quinolin-2(1H)-one (**15**).* To a suspension of **14** (600 mg, 1.82 mmol) and tetrakis-(triphenylphosphine)palladium(0) (115 mg, 0.10 mmol) in anhydrous toluene (20 mL), *Z*-tributyl(2-ethoxyethenyl)stannane (730 μL, 2.18 mmol) was added and the resulting mixture was heated and stirred at 100 °C for 8 h under N_2 atmosphere. The reaction mixture was cooled to room temperature, filtered through a pad of Celite, and evaporated. The residue was purified by flash chromatography (hexane/EtOAc 3:2) to give **15** as yellow oil (364 mg, 62% yield). IR: 3400, 3192, 3033, 2977, 2925, 1660, 1643, 1605, 1562, 1455, 1382, 1356, 1345, 1309, 1273, 1231, 1178, 1098, 1029 cm^{-1}. ^1H NMR (600 MHz, CD_3OD) δ (ppm) 1.34 (t, J = 7.1 Hz, 3H), 3.99 (q, J = 7.1 Hz, 2H), 5.18 (s, 2H), 5.53 (d, J = 7.2 Hz, 1H), 6.35 (d, J = 7.1 Hz, 1H), 6.64−6.66 (m, 1H), 7.03 (d, J = 8.5 Hz, 1H), 7.35−7.44 (m, 5H), 7.66 (d, J = 8.5 Hz, 1H), 8.01 (d, J = 9.9 Hz, 1H). ^{13}C NMR (150 MHz, CD_3OD) δ (ppm) 14.78, 69.13, 70.93, 99.48, 111.45, 117.36, 121.46, 122.82, 125.61, 127.77, 128.37, 128.48, 128.73, 128.78, 132.09, 135.74, 137.51, 142.51, 147.28, 161.59. APCI-MS m/z 322.2 [M^+ + 1]. HPLC: t_R = 20.9 min, purity 96.4%.

*2-(8-(Benzyloxy)-2-oxo-1,2-dihydroquinolin-5-yl)acetaldehyde (**16**).* To a solution of **15** (348 mg, 1.08 mmol) in acetone (2.0 mL), 2 N HCl (0.3 mL) was added and the resulting mixture was heated and stirred at reflux for 1 h. The reaction mixture was cooled to room temperature, and solvent was evaporated. The residue was dissolved in H_2O and extracted with CH_2Cl_2. The combined organic layers were dried (Na_2SO_4), filtered, and evaporated. The crude material was employed in the next reaction.

*8-(Benzyloxy)-5-(2-(propylamino)ethyl)quinolin-2(1H)-one (**17**).* To a solution of crude **16** (1.08 mmol) and *n*-propylamine (440 μL, 5.40 mmol) in anhydrous THF (15 mL), $NaBH(OAc)_3$ (370 mg, 1.72 mmol) was added and the resulting mixture was stirred for 16 h at room temperature under N_2 atmosphere. The solvent was evaporated, and saturated $NaHCO_3$ solution was added. The aqueous layer was extracted with CH_2Cl_2, and the combined organic layers were dried (Na_2SO_4), filtered, and evaporated. The residue was purified by flash chromatography (CH_2Cl_2/MeOH 98:2 + 0.2% NH_4OH) to give **17** as yellow oil (170 mg, 47% yield). IR: 3450, 2965, 1657, 1607, 1561, 1457, 1273, 1074, 840 cm^{-1}. ^1H NMR (600 MHz, CD_3OD) δ (ppm) 1.01 (t, J = 7.4 Hz, 3H), 1.66−1.75 (m, 2H), 2.95−2.97 (m, 2H), 3.15−3.25 (m, 4H), 5.33 (s, 2H), 6.72 (d, J = 9.8 Hz, 1H), 7.09 (d, J = 8.2 Hz, 1H), 7.17 (d, J = 8.2 Hz, 1H), 7.31−7.34 (m, 1H), 7.36−7.40 (m, 2H), 7.49−7.50 (m, 2H), 8.19 (d, J = 9.8 Hz, 1H). ^{13}C NMR (150 MHz, CD_3OD) δ (ppm) 11.31, 21.05, 29.72, 49.76, 50.80, 71.90, 113.77, 119.91, 122.65, 124.89, 127.41, 128.85, 129.36, 129.73, 130.79, 137.76, 138.79, 145.69, 164.16. APCI-MS m/z 337.4 [M^+ + 1]. HPLC: t_R = 15.1 min, purity 97.9%.

*N-(4-((2-(8-(Benzyloxy)-2-oxo-1,2-dihydroquinolin-5-yl)ethyl)-(propyl)amino)butyl)-4-(3-(1-butyl-1H-1,2,3-triazol-4-yl)propoxy)-3-methoxybenzamide (**18**).* To a solution of **17** (20 mg, 0.06 mmol) in THF (5 mL) and $NaBH(OAc)_3$ (64 mg, 0.30 mmol), a solution of of

DOI: 10.1021/jm501889t
J. Med. Chem. XXXX, XXX, XXX−XXX

4-(3-(1-butyl-1*H*-1,2,3-triazol-4-yl)propoxy)-*N*-(4-oxobutyl)-3-methoxybenzamide[16] (72 mg, 0.18 mmol) in THF (5 mL) was added and the reaction mixture was stirred for 18 h at room temperature under N_2 atmosphere. The solvent was evaporated, and saturated $NaHCO_3$ solution was added. The suspension was extracted with CH_2Cl_2, and the combined organic layers were dried (Na_2SO_4), filtered, and evaporated. The residue was purified by flash chromatography (CH_2Cl_2/MeOH 95:5 + 0.2% NH_4OH) to give **18** as yellow oil (31 mg, 72% yield). IR: 3307, 3015, 2936, 2869, 1659, 1605, 1580, 1505, 1464, 1268, 1228, 1129, 1053, 1032, 835 cm^{-1}. ^1H NMR (600 MHz, CD_3OD) δ (ppm) 0.86−0.96 (m, 6H), 1.22−1.38 (m, 4H), 1.54−1.66 (m, 6H), 1.80−1.88 (m, 2H), 2.12−2.19 (m, 2H), 2.73−2.78 (m, 2H), 2.85−2.92 (m, 4H), 3.07−3.15 (m, 2H), 3.39−3.41 (m, 2H), 4.07 (t, J = 6.2 Hz, 2H), 4.34 (t, J = 8.2 Hz, 2H), 5.29 (s, 2H), 6.64 (d, J = 9.7 Hz, 1H), 6.94 (d, J = 8.2 Hz, 1H), 7.01 (d, J = 8.2 Hz, 1H), 7.09 (d, J = 8.1 Hz, 1H), 7.30−7.42 (m, 5H), 7.48−7.50 (m, 2H,), 7.74 (s, 1H), 8.11 (d, J = 9.8 Hz, 1H). ^{13}C NMR (150 MHz, CD_3OD) δ (ppm) 11.68, 13.74, 20.18, 20.64, 22.88, 28.23, 30.01, 33.32, 40.19, 50.98, 54.27, 55.96, 56.54, 56.86, 69.08, 71.91, 112.21, 113.39, 113.74, 119.94, 121.70, 122.24, 123.37, 124.73, 128.09, 128.89, 129.10, 129.34, 129.73, 130.51, 137.82, 139.10, 145.20, 148.31, 150.58, 152.90, 164.17, 169.79. APCI-MS m/z 723.9 [M^+ + 1]. HPLC: t_R = 13.0 min, purity 97.4%.

*(S)-6-(Propylamino)-5,6,7,8-tetrahydronaphthalen-1-ol (**19**).* A suspension of commercially available (*S*)-5-methoxy-*N*-propyl-1,2,3,4-tetrahydronaphthalen-2-amine (200 mg, 0.91 mmol) in aqueous hydrobromic acid 48% was heated to reflux for 16 h. After the reaction was cooled to room temperature, 2N NaOH was added to adjust a pH of 9 and the mixture was extracted with CH_2Cl_2. The combined organic layers were dried (Na_2SO_4), filtered, and evaporated to give crude (*S*)-**19**, which was used in the following reaction without further purification. Crude (*R*)-**19** was prepared from (*R*)-5-methoxy-*N*-propyl-1,2,3,4-tetrahydronaphthalen-2-amine (250 mg, 1.14 mmol) as described above for (*S*)-**19**.

Receptor Binding Studies. Receptor binding studies were carried out as described previously.[17,54,55] In brief, human D_1 binding was achieved using homogenates of membranes from HEK 293 cells, which were transiently transfected with the pcDNA3.1 vector containing the appropriate human gene (from Missouri S&T cDNA Resource Center (UMR), Rolla, MO) by the calcium phosphate method.[56] Membranes were incubated at a final concentrations of 4−10 μg/well with receptor densities (B_{max} values) of 1800−3500 fmol/mg protein and a K_D value of 0.55 nM with the radioligand [^{3}H]SCH23390 (specific activity 80 Ci/mmol; Biotrend, Cologne, Germany) at 0.70 nM. The D_1 affinities for the test compounds (*R*)-**1** and (*S*)-**1** were derived with receptor preparations from porcine striatal membranes at a final protein concentration of 20−30 μg/assay tube and [^{3}H]SCH 23390 at 0.50 nM (K_D = 0.56−0.67 nM, B_{max} = 420−630 fmol/mg protein).[54] For competition binding experiments with the human D_{2L}, D_{2S},[57] D_3,[58] and $D_{4.4}$[59] receptors, preparations of membranes from CHO cells stably expressing the corresponding receptor were used together with [^{3}H]spiperone (specific activity = 81 Ci/mmol, PerkinElmer, Rodgau, Germany) at a final concentration of 0.10−0.30 nM. The assays were carried out at a protein concentration of 1−8 μg/assay tube, showing K_D values of 0.045−0.12, 0.040−0.12, 0.0958, and 0.17−0.30 nM and corresponding B_{max} values of 500−1400, 1500−4400, 11000, and 1600−2200 fmol/mg for the D_{2L}, D_{2S}, D_3, and $D_{4.4}$ receptors, respectively. Human D_5 and 5-HT_{2A} binding was achieved using homogenates of membranes from HEK 293 cells, which were transiently transfected with the pcDNA3.1 vector containing the appropriate human gene (all purchased from Missouri S&T cDNA Resource Center (UMR), Rolla, MO) by the calcium phosphate method.[56] Membranes were incubated at final concentrations of 5−10 or 4 μg/well with receptor densities (B_{max} values) of 350−1600 and 1700 fmol/mg protein and specific binding affinities (K_D values) of 0.37−0.61 and 0.40 nM for D_5 and 5-HT_{2A}, respectively. The radioligands [^{3}H]SCH23390 (specific activity 80 Ci/mmol; Biotrend, Cologne, Germany) and [^{3}H]ketanserin (specific activity 53 Ci/mmol; PerkinElmer, Rodgau, Germany) were used at concentrations of 0.50−0.60 nM for D_5 and 0.50 nM for 5-HT_{2A}, respectively. Receptor binding experiments at 5-HT_{1A} and α_1 were performed with homogenates prepared from porcine cerebral cortex.[60,61] Assays were run with membranes at a protein concentration of 60 or 20−40 μg/well, B_{max} values of 65−130 and 150−340 fmol/mg, K_D values of 0.062−0.19 and 0.075−0.10 nM, and radioligand concentrations of 0.15−0.30 nM for [^{3}H]WAY600135 (specific activity 80 Ci/mmol; Biotrend, Cologne, Germany) and 0.20 nM for [^{3}H]prazosin (specific activity 85 Ci/mmol; PerkinElmer, Rodgau, Germany) for 5-HT_{1A} and α_1 receptors, respectively. Unspecific binding was determined in the presence of haloperidol (10 μM for D_1−D_5), WAY600135 (10 μM for 5-HT_{1A}), ketanserin (10 μM for 5-HT_{2A}), or prazosin (10 μM for α_1).[60] Protein concentration was established by the method of Lowry using bovine serum albumin as standard.[62]

[^{35}S]GTPγS Incorporation Assay. The [^{35}S]GTPγS binding assay was performed using membrane preparations of transiently transfected HEK-293 cells that expressed the corresponding dopamine receptor and the appropriate pertussin toxin insensitive Gα protein (D_{2L} + $G\alpha_{o1}$, D_{2L} + $G\alpha_{i2}$, D_{2S} + $G\alpha_{o1}$, D_{2S} + $G\alpha_{i2}$) as describe previously.[55] In brief, membranes (30 μg/mL of membrane protein), compounds and 10 μM GDP were preincubated in the absence of [^{35}S]GTPγS for 30 min at 37 °C. After the addition of 0.10 nM [^{35}S]GTPγS (specific activity = 1250 Ci/mmol, PerkinElmer, Rodgau, Germany), membranes were incubated for additional 30 min (D_2 + $G\alpha_{o1}$) or 75 min (D_2 + $G\alpha_{i2}$) at 37 °C. Reactions were terminated by filtration through Whatman GF/B filters soaked with ice-cold PBS. The filter-bound radioactivity was measured as described above. Three to eight experiments per compound were performed with each concentration in triplicates.

***β*-Arrestin Recruitment Assay.** The measurement of β-arrestin-2 recruitment stimulated by receptor activation was performed by utilizing the PathHunter assay purchased from DiscoveRx (DiscoveRx, Birmingham, UK) according to the manufacturer's protocol. In brief, HEK-239 cells stably expressing the enzyme acceptor (EA)-tagged β-arrestin fusion protein were transiently transfected with the ProLink (ARMS2-PK2)-tagged dopamine receptor D_{2S} using the TransIT-293 transfection reagent from Mirus (purchased from MoBiTec, Goettingen, Germany). Cells (5000 cells per well) were seeded in 384-well plates and maintained for 24 h. After incubation with different concentrations of test compounds (from 10^{-13} to 10^{-4} M final concentration) in duplicates for 5 h, the detection mix was added and incubation was continued for further 60 min. Chemiluminescence was determined with a plate reader for microplates (Victor^3-V, PerkinElmer, Rodgau, Germany).

Data Analysis. The resulting competition curves of the receptor binding experiments were analyzed by nonlinear regression using the algorithms in PRISM 5.0 (GraphPad Software, San Diego, CA). The data were initially fit using a sigmoid model to provide an IC_{50} value, representing the concentration corresponding to 50% of maximal inhibition. IC_{50} values were transformed to K_i values according to the equation of Cheng and Prusoff.[63]

Dose−response curves for [^{35}S]GTPγS binding were normalized to basal binding of radioactivity (= 0%) and the effect of the full agonist and reference compound quinpirole (maximum effect = 100%). Three to nine curves each representing individual experiments were pooled to a mean curve from which the maximum activity (E_{max}) and the potency (EC_{50}) were derived using the algorithms in PRISM 5.0. Additionally, average values for E_{max} ± SEM and EC_{50} ± SEM were calculated from every individual curve for statistics purposes.

The amount of recruitment of β-arrestin was derived from the agonist induced increase of chemiluminescence, which was expressed in cps (counts per second). Dose−response curves were normalized to basal cps stimulated by buffer (= 0%) and the effect of the full agonist and reference compound quinpirole (maximum effect = 100%). Three to 18 curves, each representing individual experiments, were pooled to a mean curve from which the maximum activity (E_{max}) and the potency (EC_{50}) were derived using the algorithms in PRISM 5.0. Additionally, average values for E_{max} ± SEM and EC_{50} ± SEM were calculated from every individual curve for statistics purposes.

DOI: 10.1021/jm501889t
J. Med. Chem. XXXX, XXX, XXX−XXX

The operational model of agonism[34] was used to quantify ligand bias as described previously.[19,64] Dose−response curves for the agonists were fitted to the following equations by applying algorithms of PRISM 5.0.

$$Y = \text{basal} + \frac{E_m - \text{basal}}{1 + 10^{(\log EC_{50} - \log[X])}}$$

while basal describes the capacity of a the receptor to activate effector proteins in absence of an agonist, E_m the maximal response, EC_{50} denotes the concentration indicating the half-maximal effect, and $[X]$ the concentration of the agonist. Transduction coefficients $\log(\tau/K_A)$ were used to quantify the ligand bias among different signaling pathways and were obtained in their logarithmic form from

$$Y = \text{basal} + \frac{(E_m - \text{basal})\left(\frac{\tau}{K_A}\right)^n [X]^n}{\left(\frac{\tau}{K_A}\right)^n [X]^n + \left(1 + \frac{[X]}{K_A}\right)^n}$$

K_A denotes the equilibrium dissociation constant of compound (X), τ the transducer constant, and n the transducer slope. As Hill slopes were close to unity, this parameter was fixed to 1.0 throughout the analysis. Transduction coefficients were then normalized to the response of the nonbiased reference agonist quinpirole to account for cell system-dependent factors between different assay systems.

$$\Delta\log\left(\frac{\tau}{K_A}\right) = \log\left(\frac{\tau}{K_A}\right)_{\text{agonist}} - \log\left(\frac{\tau}{K_A}\right)_{\text{quinpirole}}$$

Final quantification was performed by comparison of $\Delta\Delta\log(\tau/K_A)$ between different signaling pathways at D_{2S} receptors or between signaling via $G\alpha_{o1}$ and $G\alpha_{i2}$ at D_{2L} receptors. Bias factors were calculated from bias factor = $10^{\Delta\Delta\log(\tau/KA)}$.

Molecular Docking. The test compounds (*R*)-**2**, **3**, and (*S*)-**4** were geometry optimized by means of Gaussian 09[65] at the HF/6-31(d,p) level (attributing a formal charge of +1) and docked into our recently published D_2 model[16] using AutoDock Vina[66] as described.[16] The docking results were inspected manually, and we selected one conformation of each ligand−receptor complex for further investigations. Each ligand−receptor complex was submitted to an energy minimization procedure as described.[16] The initial conformation of the (*S*)-**2**−D_2 receptor complex was derived from within our previous work by an identical docking procedure.[16] An overview of the initial, minimized conformation of each ligand−receptor complex is shown in Supporting Information, Figure S2.

Membrane Simulations. The ligand−receptor complexes were inserted into a pre-equilibrated membrane of dioleoylphosphatidylcholine (DOPC) lipids (which was built up according to a procedure successfully applied earlier)[67] by means of the GROMACS tool g_membed[68] as described.[19] The charges of the simulation systems were neutralized by adding 10 chlorine atoms to each system. In total, the simulation systems consisted of 101001 atoms, 101002 atoms, 101005 atoms, and 101003 atoms for the (*S*)-**1**-, (*R*)-**2**-, **3**-, and (*S*)-**4**-complexes. As in our previous work,[19,67] the general AMBER force field (GAFF)[69] was used for the ligands and DOPC molecules, the all-atom force field ff99SB[70] was used for D_2R, and the SPC/E water model[71] was applied. Parameters for the test compounds were assigned as described,[67] and a formal charge of +1 was defined for each test compounds. We performed two individual productive simulation runs of 100 ns for each ligand−receptor complex by means of the GROMACS simulation package[72] as described earlier,[67] thereby starting from the same initial conformation of the ligands but with different initial velocities attributed to the atoms of the simulation systems. Analysis of the trajectories was performed using the PTRAJ module of AMBER10,[73] and figures were prepared using UCSF Chimera.[74]

■ ASSOCIATED CONTENT

Supporting Information

^1H and ^{13}C NMR spectra, results of functional assays, calculations, overview over simulation systems, docking results, analysis of MD simulations (RMSD, distance plots). This material is available free of charge via the Internet at http://pubs.acs.org.

■ AUTHOR INFORMATION

Corresponding Author

*Phone: +49 9131 85-29383. Fax: +49 9131 85-22585. E-mail: peter.gmeiner@fau.de.

Notes

The authors declare no competing financial interest.

■ ACKNOWLEDGMENTS

This work was supported by grants from the German Research Foundation (Deutsche Forschungsgemeinschaft Gm 13/10, GRK 1910). We thank Graeme Milligan (University of Glasgow, U.K.) for providing us with the cDNA for $G\alpha_{o1}$ and $G\alpha_{i2}$ proteins, and Nuska Tschammer, Stefan Schuster, and Tamara Schellhorn for the construction of D_2 mutants and the ARMS2-PK2-tagged D_{2S} receptor cDNA. We also thank Dorothée Möller for helpful discussions.

■ ABBREVIATIONS USED

aripiprazole, 7-[4-[4-(2,3-dichlorophenyl)piperazin-1-yl]-butoxy]-3,4-dihydroquinolin-2(1*H*)-one; D_x, dopamine D_x receptor; 5-HT_{xx}, 5-hydroxytryptamin$_{xx}$ receptor subtype; GTPγS, guanosine 5′-*O*-(thiotriphosphate); spiperone, 8-[4-(4-fluorophenyl)-4-oxobutyl]-1-phenyl-1,3,8-triazaspiro[4.5]-decan-4-one; HEK, human embryonic kidney; CHO, chinese hamster ovary; SEM, standard error of mean; ketanserin, 3-[2-[4-(4-fluorobenzoyl)piperidin-1-yl]ethyl]quinazoline-2,4-(1*H*,3*H*)-dione; prazosin, 2-[4-(2-furoyl)piperazin-1-yl]-6,7-dimethoxyquinazolin-4-amine; PTX, pertussis toxin; quinpirole, (4a*R*-*trans*)-4,4a,5,6,7,8,8a,9-octahydro-5-propyl-1*H*-pyrazolo-[3,4-g]quinoline; SCH23390, 7-chloro-8-hydroxy-3-methyl-1-phenyl-2,3,4,5-tetrahydro-1*H*-3-benzazepine hydrochloride; WAY100135, *N*-*tert*-butyl-3-(4-(2-methoxyphenyl)-piperazin-1-yl)-2-phenylpropan-amide dihydrochloride; 5OH-DPAT, 5-hydroxy-*N*,*N*-dipropyl-2-amino-tetraline; APCI, atmospheric pressure chemical ionization; ESI, electron-spray ionization; $LiAlH_4$, lithium aluminum hydride; TMS, trimethylsilyl; TBTU, *O*-(benzotriazol-1-yl)-*N*,*N*,*N*′,*N*′-tetramethyluronium tetrafluoroborate; 1,4-DAP, 1,4-disubstituted-aromatic piperazine; RMSD, root-mean-square deviation; MD, molecular dynamics; EL, extracellular loop; TM, transmembrane helix

■ REFERENCES

(1) Schizophrenia Working Group of the Psychiatric Genomics Consortium.. Biological insights from 108 schizophrenia-associated genetic loci. *Nature* **2014**, *511*, 421−427.

(2) Davis, K. L.; Kahn, R. S.; Ko, G.; Davidson, M. Dopamine in schizophrenia: a review and reconceptualization. *Am. J. Psychiatry* **1991**, *148*, 1474−1486.

(3) Beaulieu, J.-M.; Gainetdinov, R. R. The physiology, signaling, and pharmacology of dopamine receptors. *Pharmacol. Rev.* **2011**, *63*, 182−217.

(4) Ye, N.; Neumeyer, J. L.; Baldessarini, R. J.; Zhen, X.; Zhang, A. Update 1 of: Recent progress in development of dopamine receptor subtype-selective agents: potential therapeutics for neurological and psychiatric disorders. *Chem. Rev.* **2013**, *113*, PR123−PR178.

DOI: 10.1021/jm501889t
J. Med. Chem. XXXX, XXX, XXX−XXX

(5) Lindgren, N.; Usiello, A.; Goiny, M.; Haycock, J.; Erbs, E.; Greengard, P.; Hökfelt, T.; Borrelli, E.; Fisone, G. Distinct roles of dopamine D2L and D2S receptor isoforms in the regulation of protein phosphorylation at presynaptic and postsynaptic sites. *Proc. Natl. Acad. Sci. U. S. A.* **2003**, *100*, 4305−4309.
(6) Gazi, L.; Nickolls, S. A.; Strange, P. G. Functional coupling of the human dopamine D2 receptor with Gαi1, Gαi2, Gαi3 and Gαo G proteins: evidence for agonist regulation of G protein selectivity. *Br. J. Pharmacol.* **2003**, *138*, 775−786.
(7) Urban, J. D.; Clarke, W. P.; von Zastrow, M.; Nichols, D. E.; Kobilka, B.; Weinstein, H.; Javitch, J. A.; Roth, B. L.; Christopoulos, A.; Sexton, P. M.; Miller, K. J.; Spedding, M.; Mailman, R. B. Functional selectivity and classical concepts of quantitative pharmacology. *J. Pharmacol. Exp. Ther.* **2007**, *320*, 1−13.
(8) Neve, K. A. *Functional Selectivity of G Protein-Coupled Receptor Ligands—New Opportunities for Drug Discovery*, 1st ed.; Humana Press: Totowa, NJ, 2009; pp 25−40.
(9) Rajagopal, K.; Lefkowitz, R. J.; Rockman, H. A. When 7 transmembrane receptors are not G protein-coupled receptors. *J. Clin. Invest.* **2005**, *115*, 2971−2974.
(10) Masri, B.; Salahpour, A.; Didriksen, M.; Ghisi, V.; Beaulieu, J.-M.; Gainetdinov, R. R.; Caron, M. G. Antagonism of dopamine D2 receptor/β-arrestin 2 interaction is a common property of clinically effective antipsychotics. *Proc. Natl. Acad. Sci. U. S. A.* **2008**, *105*, 13656−13661.
(11) Allen, J. A.; Yost, J. M.; Setola, V.; Chen, X.; Sassano, M. F.; Chen, M.; Peterson, S.; Yadav, P. N.; Huang, X.-p.; Feng, B.; Jensen, N. H.; Che, X.; Bai, X.; Frye, S. V.; Wetsel, W. C.; Caron, M. G.; Javitch, J. A.; Roth, B. L.; Jin, J. Discovery of β-arrestin-biased dopamine D2 ligands for probing signal transduction pathways essential for antipsychotic efficacy. *Proc. Natl. Acad. Sci. U. S. A.* **2011**, *108*, 18488−18493.
(12) Chen, X.; Sassano, M. F.; Zheng, L.; Setola, V.; Chen, M.; Bai, X.; Frye, S. V.; Wetsel, W. C.; Roth, B. L.; Jin, J. Structure−functional selectivity relationship studies of beta-arrestin-biased dopamine D(2) receptor agonists. *J. Med. Chem.* **2012**, *55*, 7141−7153.
(13) Shonberg, J.; Herenbrink, C. K.; López, L.; Christopoulos, A.; Scammells, P. J.; Capuano, B.; Lane, J. R. A Structure−activity analysis of biased agonism at the dopamine D2 receptor. *J. Med. Chem.* **2013**, *56*, 9199−9221.
(14) Szabo, M.; Klein Herenbrink, C.; Christopoulos, A.; Lane, J. R.; Capuano, B. Structure−activity relationships of privileged structures lead to the discovery of novel biased ligands at the dopamine D2 receptor. *J. Med. Chem.* **2014**, *57*, 4924−4939.
(15) Dörfler, M.; Tschammer, N.; Hamperl, K.; Hübner, H.; Gmeiner, P. Novel D3 selective dopaminergics incorporating enyne units as nonaromatic catechol bioisosteres: synthesis, bioactivity, and mutagenesis studies. *J. Med. Chem.* **2008**, *51*, 6829−6838.
(16) Hiller, C.; Kling, R. C.; Heinemann, F. W.; Meyer, K.; Hubner, H.; Gmeiner, P. Functionally selective dopamine D2/D3 receptor agonists comprising an enyne moiety. *J. Med. Chem.* **2013**, *56*, 5130−5141.
(17) Tschammer, N.; Elsner, J.; Goetz, A.; Ehrlich, K.; Schuster, S.; Ruberg, M.; Kühhorn, J.; Thompson, D.; Whistler, J.; Hübner, H.; Gmeiner, P. Highly potent 5-aminotetrahydropyrazolopyridines: enantioselective dopamine D3 receptor binding, functional selectivity, and analysis of receptor−ligand interactions. *J. Med. Chem.* **2011**, *54*, 2477−2491.
(18) Tschammer, N.; Bollinger, S.; Kenakin, T.; Gmeiner, P. Histidine 6.55 is a major determinant of ligand-biased signaling in dopamine D2L receptor. *Mol. Pharmacol.* **2011**, *79*, 575−585.
(19) Möller, D.; Kling, R. C.; Skultety, M.; Leuner, K.; Hübner, H.; Gmeiner, P. Functionally selective dopamine D2, D3 receptor partial agonists. *J. Med. Chem.* **2014**, *57*, 4861−4875.
(20) Wacker, D.; Wang, C.; Katritch, V.; Han, G. W.; Huang, X. P.; Vardy, E.; McCorvy, J. D.; Jiang, Y.; Chu, M.; Siu, F. Y.; Liu, W.; Xu, H. E.; Cherezov, V.; Roth, B. L.; Stevens, R. C. Structural features for functional selectivity at serotonin receptors. *Science* **2013**, *340*, 615−619.
(21) Wang, C.; Jiang, Y.; Ma, J.; Wu, H.; Wacker, D.; Katritch, V.; Han, G. W.; Liu, W.; Huang, X.-P.; Vardy, E.; McCorvy, J. D.; Gao, X.; Zhou, X. E.; Melcher, K.; Zhang, C.; Bai, F.; Yang, H.; Yang, L.; Jiang, H.; Roth, B. L.; Cherezov, V.; Stevens, R. C.; Xu, H. E. Structural basis for molecular recognition at serotonin receptors. *Science* **2013**, *340*, 610−614.
(22) Kaiser, C.; Dandridge, P. A.; Garvey, E.; Flaim, K. E.; Zeid, R. L.; Hieble, J. P. Dopamine receptor agonist activity of some 5-(2-aminoethyl)carbostyril derivatives. *J. Med. Chem.* **1985**, *28*, 1803−1810.
(23) Cannon, J. G. Structure−activity relationships of dopamine agonists. *Annu. Rev. Pharmacol. Toxicol.* **1983**, *23*, 103−129.
(24) Elsner, J.; Boeckler, F.; Heinemann, F. W.; Hübner, H.; Gmeiner, P. Pharmacophore-guided drug discovery investigations leading to bioactive 5-aminotetrahydropyrazolopyridines. Implications for the binding mode of heterocyclic dopamine D3 receptor agonists. *J. Med. Chem.* **2005**, *48*, 5771−5779.
(25) Wiens, B. L.; Nelson, C. S.; Neve, K. A. Contribution of serine residues to constitutive and agonist-induced signaling via the D2S dopamine receptor: evidence for multiple, agonist-specific active conformations. *Mol. Pharmacol.* **1998**, *54*, 435−444.
(26) Coley, C.; Woodward, R.; Johansson, A. M.; Strange, P. G.; Naylor, L. H. Effect of multiple serine/alanine mutations in the transmembrane spanning region V of the D2 dopamine receptor on ligand binding. *J. Neurochem.* **2000**, *74*, 358−366.
(27) Shimizu, T.; Murakoshi, K.; Yasui, K.; Sodeoka, M. A new route for the preparation of succinates. *Synthesis* **2008**, *20*, 3209−3218.
(28) Koide, M.; Kume, K. Preparation of [(trifluoromethyl)phenyl]-acetic acids from (trifluoromethyl)benzenes and vinyl compounds. JP2001302582A, 2001.
(29) Shenoy, S. K.; Drake, M. T.; Nelson, C. D.; Houtz, D. A.; Xiao, K.; Madabushi, S.; Reiter, E.; Premont, R. T.; Lichtarge, O.; Lefkowitz, R. J. β-Arrestin-dependent G Protein-independent ERK1/2 activation by the β2 adrenergic receptor. *J. Biol. Chem.* **2006**, *281*, 1261−1273.
(30) Shonberg, J.; Lopez, L.; Scammells, P. J.; Christopoulos, A.; Capuano, B.; Lane, J. R. Biased agonism at G protein-coupled receptors: the promise and the challenges—a medicinal chemistry perspective. *Med. Res. Rev.* **2014**, *34*, 1286−1330.
(31) Senogles, S. E. The D2 dopamine receptor isoforms signal through distinct Gi alpha proteins to inhibit adenylyl cyclase. A study with site-directed mutant Gi alpha proteins. *J. Biol. Chem.* **1994**, *269*, 23120−23127.
(32) Wise, A.; Watson-Koken, M. A.; Rees, S.; Lee, M.; Milligan, G. Interactions of the alpha2A-adrenoceptor with multiple Gi-family G-proteins: Studies with pertussis toxin-resistant G-protein mutants. *Biochem. J.* **1997**, *321*, 721−728.
(33) Pauwels, P. J.; Tardif, S.; Wurch, T.; Colpaert, F. C. Facilitation of constitutive α2A-adrenoceptor activity by both single amino acid mutation (Thr373Lys) and Gαo protein coexpression: evidence for inverse agonism. *J. Pharmacol. Exp. Ther.* **2000**, *292*, 654−663.
(34) Black, J. W.; Leff, P. Operational models of pharmacological agonism. *Proc. R. Soc. B* **1983**, *220*, 141−162.
(35) Kenakin, T.; Watson, C.; Muniz-Medina, V.; Christopoulos, A.; Novick, S. A simple method for quantifying functional selectivity and agonist bias. *ACS Chem. Neurosci.* **2011**, *3*, 193−203.
(36) Kenakin, T.; Christopoulos, A. Measurements of ligand bias and functional affinity. *Nature Rev. Drug Discovery* **2013**, *12*, 483−483.
(37) Kenakin, T.; Christopoulos, A. Signalling bias in new drug discovery: detection, quantification and therapeutic impact. *Nature Rev. Drug Discovery* **2013**, *12*, 205−216.
(38) Wikstroem, H.; Andersson, B.; Sanchez, D.; Lindberg, P.; Arvidsson, L. E.; Johansson, A. M.; Nilsson, J. L. G.; Svensson, K.; Hjorth, S.; Carlsson, A. Resolved monophenolic 2-aminotetralins and 1,2,3,4,4a,5,6,10b-octahydrobenzo[*f*]quinolines: structural and stereochemical considerations for centrally acting pre- and postsynaptic dopamine-receptor agonists. *J. Med. Chem.* **1985**, *28*, 215−225.
(39) Liu, J. J.; Horst, R.; Katritch, V.; Stevens, R. C.; Wuthrich, K. Biased signaling pathways in beta2-adrenergic receptor characterized by 19F-NMR. *Science* **2012**, *335*, 1106−1110.

DOI: 10.1021/jm501889t
J. Med. Chem. XXXX, XXX, XXX−XXX

(40) Warne, T.; Edwards, P. C.; Leslie, A. G.; Tate, C. G. Crystal structures of a stabilized beta1-adrenoceptor bound to the biased agonists bucindolol and carvedilol. *Structure* **2012**, *20*, 841−849.
(41) Rahmeh, R.; Damian, M.; Cottet, M.; Orcel, H.; Mendre, C.; Durroux, T.; Sharma, K. S.; Durand, G.; Pucci, B.; Trinquet, E.; Zwier, J. M.; Deupi, X.; Bron, P.; Banères, J.-L.; Mouillac, B.; Granier, S. Structural insights into biased G protein-coupled receptor signaling revealed by fluorescence spectroscopy. *Proc. Natl. Acad. Sci. U. S. A.* **2012**, *109*, 6733−6738.
(42) Correll, C. C.; McKittrick, B. A. Biased ligand modulation of seven transmembrane receptors (7TMRs): functional implications for drug discovery. *J. Med. Chem.* **2014**, *16*, 6887−6896.
(43) Violin, J. D.; DeWire, S. M.; Yamashita, D.; Rominger, D. H.; Nguyen, L.; Schiller, K.; Whalen, E. J.; Gowen, M.; Lark, M. W. Selectively engaging β-arrestins at the angiotensin II type 1 receptor reduces blood pressure and increases cardiac performance. *J. Pharmacol. Exp. Ther.* **2010**, *335*, 572−579.
(44) Groer, C. E.; Tidgewell, K.; Moyer, R. A.; Harding, W. W.; Rothman, R. B.; Prisinzano, T. E.; Bohn, L. M. An opioid agonist that does not induce μ-opioid receptor−arrestin interactions or receptor internalization. *Mol. Pharmacol.* **2007**, *71*, 549−557.
(45) Bromberg, K. D.; Iyengar, R.; He, J. C. Regulation of neurite outgrowth by Gi/o signaling pathways. *Front. Biosci.* **2008**, *13*, 4544−4557.
(46) Nakata, H.; Kozasa, T. Functional characterization of Gαo signaling through G protein-regulated inducer of neurite outgrowth 1. *Mol. Pharmacol.* **2005**, *67*, 695−702.
(47) Strittmatter, S. M.; Fishman, M. C.; Zhu, X. P. Activated mutants of the alpha subunit of G(o) promote an increased number of neurites per cell. *J. Neurosci.* **1994**, *14*, 2327−2338.
(48) Hwangpo, T. A.; Jordan, J. D.; Premsrirut, P. K.; Jayamaran, G.; Licht, J. D.; Iyengar, R.; Neves, S. R. G protein-regulated inducer of neurite outgrowth (GRIN) modulates sprouty protein repression of mitogen-activated protein kinase (MAPK) activation by growth factor stimulation. *J. Biol. Chem.* **2012**, *287*, 13674−13685.
(49) Allen, J. A.; Yost, J. M.; Setola, V.; Chen, X.; Sassano, M. F.; Chen, M.; Peterson, S.; Yadav, P. N.; Huang, X. P.; Feng, B.; Jensen, N. H.; Che, X.; Bai, X.; Frye, S. V.; Wetsel, W. C.; Caron, M. G.; Javitch, J. A.; Roth, B. L.; Jin, J. Discovery of beta-arrestin-biased dopamine D2 ligands for probing signal transduction pathways essential for antipsychotic efficacy. *Proc. Natl. Acad. Sci. U. S. A.* **2011**, *108*, 18488−18493.
(50) Kühhorn, J.; Götz, A.; Hübner, H.; Thompson, D.; Whistler, J.; Gmeiner, P. Development of a bivalent dopamine D2 receptor agonist. *J. Med. Chem.* **2011**, *54*, 7911−7919.
(51) Davidov, E.; Spiegelstein-Klarfeld, H.; Gizri-Yaron, O.; Naim, E.; Lichtenstein, N. New Derivatives of L-glutamine. *Isr. J. Chem.* **1969**, *7*, 487−489.
(52) Hansen, S. G.; Jensen, H. H. Microwave irradiation as an effective means of synthesizing unsubstituted N-linked 1,2,3-triazoles from vinyl acetate and azides. *Synlett* **2009**, *20*, 3275−3278.
(53) Rosenbaum, D. M.; Zhang, C.; Lyons, J. A.; Holl, R.; Aragao, D.; Arlow, D. H.; Rasmussen, S. G.; Choi, H. J.; Devree, B. T.; Sunahara, R. K.; Chae, P. S.; Gellman, S. H.; Dror, R. O.; Shaw, D. E.; Weis, W. I.; Caffrey, M.; Gmeiner, P.; Kobilka, B. K. Structure and function of an irreversible agonist-beta(2) adrenoceptor complex. *Nature* **2011**, *469*, 236−240.
(54) Hubner, H.; Haubmann, C.; Utz, W.; Gmeiner, P. Conjugated enynes as nonaromatic catechol bioisosteres: synthesis, binding experiments, and computational studies of novel dopamine receptor agonists recognizing preferentially the D-3 subtype. *J. Med. Chem.* **2000**, *43*, 756−762.
(55) Tschammer, N.; Elsner, J.; Goetz, A.; Ehrlich, K.; Schuster, S.; Ruberg, M.; Kuhhorn, J.; Thompson, D.; Whistler, J.; Hubner, H.; Gmeiner, P. Highly potent 5-aminotetrahydropyrazolopyridines: enantioselective dopamine D3 receptor binding, functional selectivity, and analysis of receptor-ligand interactions. *J. Med. Chem.* **2011**, *54*, 2477−2491.
(56) Hayes, G.; Biden, T. J.; Selbie, L. A.; Shine, J. Structural subtypes of the dopamine D2 receptor are functionally distinct: Expression of the cloned D2A and D2B subtypes in a heterologous cell line. *Mol. Endocrinol.* **1992**, *6*, 920−926.
(57) Sokoloff, P.; Giros, B.; Martres, M. P.; Bouthenet, M. L.; Schwartz, J. C. Molecular cloning and characterization of a novel dopamine receptor (D3) as a target for neuroleptics. *Nature* **1990**, *347*, 146−151.
(58) Asghari, V.; Sanyal, S.; Buchwaldt, S.; Paterson, A.; Jovanovic, V.; Van Tol, H. H. Modulation of intracellular cyclic AMP levels by different human dopamine D4 receptor variants. *J. Neurochem.* **1995**, *65*, 1157−1165.
(59) Jordan, M.; Schallhorn, A.; Wurm, F. M. Transfecting mammalian cells: optimization of critical parameters affecting calcium-phosphate precipitate formation. *Nucleic Acids Res.* **1996**, *24*, 596−601.
(60) Huebner, H.; Haubmann, C.; Utz, W.; Schmidt, S.; Schmidt, R.; Gmeiner, P. Conjugated enynes as nonaromatic catechol bioisosteres: synthesis, binding experiments, and computational studies of novel dopamine receptor agonists recognizing preferentially the D3 subtype. *J. Med. Chem.* **2000**, *43*, 756−762.
(61) Bettinetti, L.; Schlotter, K.; Hübner, H.; Gmeiner, P. Interactive SAR studies: rational discovery of super-potent and highly selective dopamine D3 receptor antagonists and partial agonists. *J. Med. Chem.* **2002**, *45*, 4594−4597.
(62) Lowry, O. H.; Rosebrough, N. J.; Farr, A. L.; Randall, R. J. Protein measurement with the folin phenol reagent. *J. Biol. Chem.* **1951**, *193*, 265−275.
(63) Cheng, Y.-C.; Prusoff, W. H. Relation between the inhibition constant (K1) and the concentration of inhibitor which causes fifty per cent inhibition (I50) of an enzymic reaction. *Biochem. Pharmacol.* **1973**, *22*, 3099−3108.
(64) Shonberg, J.; Herenbrink, C. K.; Lopez, L.; Christopoulos, A.; Scammells, P. J.; Capuano, B.; Lane, J. R. A structure−activity analysis of biased agonism at the dopamine D2 receptor. *J. Med. Chem.* **2013**, *56*, 9199−221.
(65) Frisch, M. J.; Trucks, G. W.; Schlegel, H. B.; Scuseria, G. E.; Robb, M. A.; Cheeseman, J. R.; Scalmani, G.; Barone, V.; Mennucci, B.; Petersson, G. A.; Nakatsuji, H.; Caricato, M.; Li, X.; Hratchian, H. P.; Izmaylov, A. F.; Bloino, J.; Zheng, G.; Sonnenberg, J. L.; Hada, M.; Ehara, M.; Toyota, K.; Fukuda, R.; Hasegawa, J.; Ishida, M.; Nakajima, T.; Honda, Y.; Kitao, O.; Nakai, H.; Vreven, T.; Montgomery, J. A.; Peralta, J. E.; Ogliaro, F.; Bearpark, M.; Heyd, J. J.; Brothers, E.; Kudin, K. N.; Staroverov, V. N.; Kobayashi, R.; Normand, J.; Raghavachari, K.; Rendell, A.; Burant, J. C.; Iyengar, S. S.; Tomasi, J.; Cossi, M.; Rega, N.; Millam, J. M.; Klene, M.; Knox, J. E.; Cross, J. B.; Bakken, V.; Adamo, C.; Jaramillo, J.; Gomperts, R.; Stratmann, R. E.; Yazyev, O.; Austin, A. J.; Cammi, R.; Pomelli, C.; Ochterski, J. W.; Martin, R. L.; Morokuma, K.; Zakrzewski, V. G.; Voth, G. A.; Salvador, P.; Dannenberg, J. J.; Dapprich, S.; Daniels, A. D.; Farkas; Foresman, J. B.; Ortiz, J. V.; Cioslowski, J.; Fox, D. J. *Gaussian 09*, revision B.01; Gaussian: Wallingford CT, 2009.
(66) Trott, O.; Olson, A. J. AutoDock Vina: Improving the speed and accuracy of docking with a new scoring function, efficient optimization, and multithreading. *J. Comput. Chem.* **2010**, *31*, 455−461.
(67) Goetz, A.; Lanig, H.; Gmeiner, P.; Clark, T. Molecular dynamics simulations of the effect of the G-protein and diffusible ligands on the β2-adrenergic receptor. *J. Mol. Biol.* **2011**, *414*, 611−623.
(68) Wolf, M. G.; Hoefling, M.; Aponte-Santamaria, C.; Grubmuller, H.; Groenhof, G. G_membed: efficient insertion of a membrane protein into an equilibrated lipid bilayer with minimal perturbation. *J. Comput. Chem.* **2010**, *31*, 2169−2174.
(69) Wang, J.; Wolf, R. M.; Caldwell, J. W.; Kollman, P. A.; Case, D. A. Development and testing of a General Amber force field. *J. Comput. Chem.* **2004**, *25*, 1157−1174.
(70) Hornak, V.; Abel, R.; Okur, A.; Strockbine, B.; Roitberg, A.; Simmerling, C. Comparison of multiple amber force fields and

DOI: 10.1021/jm501889t
J. Med. Chem. XXXX, XXX, XXX−XXX

development of improved protein backbone parameters. *Proteins* **2006**, *65*, 712−725.
(71) Berendsen, H. J. C.; Grigera, J. R.; Straatsma, T. P. The missing term in effective pair potentials. *J. Phys. Chem.* **1987**, *91*, 6269−6271.
(72) Van Der Spoel, D.; Lindahl, E.; Hess, B.; Groenhof, G.; Mark, A. E.; Berendsen, H. J. GROMACS: fast, flexible, and free. *J. Comput. Chem.* **2005**, *26*, 1701−1718.
(73) Case, D. A.; Darden, T. A.; Cheatham, T. E., III; Simmerling, C. L.; Wang, J.; Duke, R. E.; Luo, R.; Crowley, M.; Walker, R. C.; Zhang, W.; Merz, K. M.; Wang, B.; Hayik, S.; Roitberg, A.; Seabra, G.; Kolossváry, I.; Wong, K. F.; Paesani, F.; Vanicek, J.; Wu, X.; Brozell, S. R.; Steinbrecher, T.; Gohlke, H.; Yang, L.; Tan, C.; Mongan, J.; Hornak, V.; Cui, G.; Mathews, D. H.; Seetin, M. G.; Sagui, C.; Babin, V.; Kollman, P. A. *AMBER 10*; University of California, San Francisco: San Francisco, CA,2008.
(74) Pettersen, E. F.; Goddard, T. D.; Huang, C. C.; Couch, G. S.; Greenblatt, D. M.; Meng, E. C.; Ferrin, T. E. UCSF Chimera—a visualization system for exploratory research and analysis. *J. Comput. Chem.* **2004**, *25*, 1605−1612.

DOI: 10.1021/jm501889t
J. Med. Chem. XXXX, XXX, XXX−XXX